minerals

MDPI

Article

Impact of Diagenesis on the Low Permeability Sandstone Reservoir: Case Study of the Lower Jurassic Reservoir in the Niudong Area, Northern Margin of Qaidam Basin

Wenhuan Li [1,2], Tailiang Fan [1,2,*], Zhiqian Gao [1,2], Zhixiong Wu [3], Ya'nan Li [3], Xinlei Zhang [1,2], Heng Zhang [1,2] and Fangda Cao [1,2]

[1] School of Energy Resources, China University of Geosciences, Beijing 100083, China; 3006170006@cugb.edu.cn (W.L.); gzq@cugb.edu.cn (Z.G.); cugbbj0317@163.com (X.Z.); zhhhpu@163.com (H.Z.); chenwei2007013@163.com (F.C.)

[2] Key Laboratory of Marine Reservoir Evolution and Hydrocarbon Enrichment Mechanism, Ministry of Education, China University of Geosciences, Beijing 100083, China

[3] Research Institute of Exploration and Development of Qinghai Oilfield Company, PetroChina, Dunhuang 736202, China; wuzxqh@petrochina.com.cn (Z.W.); lynyjyqh@petrochina.com.cn (Y.L.)

* Correspondence: fantl@cugb.edu.cn

Abstract: The Lower Jurassic reservoir in the Niudong area of the northern margin of Qaidam Basin is a typical low permeability sandstone reservoir and an important target for oil and gas exploration in the northern margin of the Qaidam Basin. In this paper, casting thin section analysis, scanning electron microscopy, X-ray diffraction, and stable isotope analysis among other methods were used to identify the diagenetic characteristics and evolution as well as the main factors influencing reservoir quality in the study area. The predominant types of sandstone in the study area are mainly feldspathic lithic sandstone and lithic arkose, followed by feldspathic sandstone and lithic sandstone. Reservoir porosity ranges from 0.01% to 19.5% (average of 9.9%), and permeability ranges from 0.01 to 32.4 mD (average of 3.8 mD). The reservoir exhibits robust heterogeneity and its quality is mainly influenced by diagenesis. The Lower Jurassic reservoir in the study area has undergone complex diagenesis and reached the middle diagenesis stage (A–B). The quantitative analysis of pore evolution showed that the porosity loss rate caused by compaction and cementation was 69.0% and 25.7% on average, and the porosity increase via dissolution was 4.8% on average. Compaction was the main cause of the reduction in the physical property of the reservoir in the study area, while cementation and dissolution were the main causes of reservoir heterogeneity. Cementation can reduce reservoir space by filling primary intergranular pores and secondary dissolved pores via cementation such as a calcite and illite/smectite mixed layer, whereas high cement content increased the compaction resistance of particles to preserve certain primary pores. $\delta^{13}C$ and $\delta^{18}O$ isotopes showed that the carbonate cement in the study area was the product of hydrocarbon generation by organic matter. The study area has conditions that are conductive to strong dissolution and mainly occur in feldspar dissolution, which produces a large number of secondary pores. It is important to improve the physical properties of the reservoir. Structurally, the Niudong area is a large nose uplift structure with developed fractures, which can be used as an effective oil and gas reservoir space and migration channel. In addition, the existence of fractures provides favorable conditions for the uninterrupted entry of acid fluid into the reservoir, promoting the occurrence of dissolution, and ultimately improves the physical properties of reservoirs, which is mainly manifested in improving the reservoir permeability.

Keywords: porosity evolution; diagenesis; the low permeability sandstone reservoir; Niudong area; Qaidam Basin

Citation: Li, W.; Fan, T.; Gao, Z.; Wu, Z.; Li, Y.; Zhang, X.; Zhang, H.; Cao, F. Impact of Diagenesis on the Low Permeability Sandstone Reservoir: Case Study of the Lower Jurassic Reservoir in the Niudong Area, Northern Margin of Qaidam Basin. *Minerals* **2021**, *11*, 453. https://doi.org/10.3390/min11050453

Academic Editor: Ricardo Ferreira Louro Silva

Received: 15 March 2021
Accepted: 22 April 2021
Published: 25 April 2021

1. Introduction

Following the increasing demand for oil and gas in various countries and the increasing difficulty in developing conventional reservoirs, the exploration and development of

unconventional reservoirs has become increasingly important [1]. As a kind of unconventional oil and gas reservoir, low permeability reservoirs are rich in oil and gas resources and are widely distributed in North America, Central Asia, East Asia, Southeast Asia, and Northern Europe, among other places [2–5]. Approximately 38% of the world's oil and gas resources are currently in low permeability reservoirs, and in China, the proportion is as high as 46% [6,7]. In 1871, the famous Bradford Oilfield was discovered in the United States, and this discovery initiated the exploration and research of low permeability reservoirs in foreign countries [8,9]. However, the exploration and development of low permeability reservoirs in China started from the successful development of the Ansai Oilfield in 1995 [6,10]. At present, low permeability reservoirs have been identified in many petroliferous basins in China, which are mainly distributed in the Dongliao Basin, Bohai Bay Basin, Jianghan Basin, Hailar Basin, Ordos Basin, Sichuan Basin, Junggar Basin, Tarim Basin, and Qaidam Basin [10–13]. By the end of 2016, low-permeability reservoirs accounted for 12% of confirmed petroleum reserves in China, and 39% of the cumulatively verified natural gas reserves in China [6]. Low permeability sandstone reservoirs have become one of the important options for oil and gas exploration and development in China [10,14,15].

The quality of reservoirs determines whether industrial reservoirs can be formed, which is especially important for low permeability reservoirs [16–19]. Generally, reservoirs with permeability that is below 50 mD are referred to as low permeability reservoirs [5,14,20]. They exhibit inferior low permeability, strong heterogeneity, small pore throat radius, low productivity, large diagenetic difference, and relatively developed fractures among other characteristics [4,5,15,21].

The formation of low permeability reservoirs is controlled by regional sedimentary background and complex diagenesis [20,22,23]. The sedimentary environment controls the mineral composition, grain size, sorting, and grinding of the original sandstone, which determines the original porosity and permeability of the reservoir [15,24,25], and strongly affects subsequent diagenetic evolution [26].

Diagenesis plays an extremely important role in the formation of low permeability reservoirs. Meanwhile, the study of diagenetic process reveals its influence on the evolution of reservoir quality and elucidates the formation mechanism of low permeability reservoirs [15,27]. Based on its influence on reservoir quality, the diagenetic process can be divided into constructive diagenesis (favorable for the preservation of pore throat) and destructive diagenesis (unfavorable for the preservation of pore throat and reducing the physical properties of the reservoir) [27–29]. These can be subdivided into compaction, cementation (carbonate cementation, clay mineral cementation, siliceous cementation, etc.), dissolution (dissolution of clastic particles, dissolution of interstitial materials), metasomatism, and microcracks (stress joints and chemical dissolution cracks caused by mechanical compaction, etc.) [18]. Compaction is generally considered to be the main factor affecting the loss of the original porosity of sandstone [21], while the influence of cementation on reservoir physical properties has two effects. On one hand, cementation between particles can improve the pressure resistance of the reservoir and alleviate some of the compaction, which is beneficial to the preservation of primary pores. On the other hand, cementing materials reduce the physical properties of the reservoir by filling intergranular and intragranular pores [30,31]. Dissolution can generally improve the physical properties of the reservoir to a certain extent [32,33]. Most low-permeability reservoirs in China such as the low-permeability sandstone in Ordos Basin and Niudong area discussed in this paper are deposited in delta deposits and are closely related to coal measure strata [20,34]. The sedimentary environment of the coal measure strata is rich in aquatic and terrestrial plants. After the deposition of sediments, the plants isolate from the water and decompose to produce humic acid, which makes the formation water acidic [15]. The acidic environment can promote the formation of cements such as quartz overgrowth and kaolinite, and also lay the foundation for the ultimate dissolution [15,34,35].

According to formation reasons, low-permeability reservoirs can be divided into primary low-permeability reservoirs and secondary low-permeability reservoirs [20]. The primary low-permeability reservoirs are mainly affected by sedimentation and feature shallow burials, predominant primary pores, and undeveloped fractures whereas secondary low-permeability sandstone reservoirs have undergone complex diagenetic transformation and are buried deep. Most of the low-permeability reservoirs discovered in China are categorized under secondary low-permeability reservoirs [15].

The Lower Jurassic sandstone in the Niudong area on the northern margin of the Qaidam Basin is a typical secondary low permeability reservoir. The discovery of the Niudong gas field is an indication of the important exploration value of the area. The Lower Jurassic reservoir in the Niudong area has undergone various types of diagenetic stages, and information on its diagenetic characteristics and pore evolution process provides significant guidelines for exploration and development. However, previous studies on the Niudong area only involve structural characteristics [36], and many research studies have investigated the northern margin holistically [37,38]. Only a small number of scholars have investigated the diagenetic characteristics and factors influencing the Lower Jurassic reservoir in the Niudong area of the northern margin of Qaidam, therefore, information on this topic is insufficient [39].

Based on previous studies through petrological and mineralogical analysis methods such as core observation, casting thin section, scanning electron microscopy, determination of porosity and permeability, X-ray, stable isotope analysis, and organic matter maturity, this paper investigated and quantitative or semi-quantitative analyzed the influencing factors of the low permeability reservoir of the Lower Jurassic in the Niudong area in the northern margin of Qaidam Basin. The objectives of this paper are as follows:

(1) to clarify the detrital composition, structure, cementation, pore structure, and physical properties of the Lower Jurassic reservoir in the Niudong area;

(2) to study the types and characteristics of diagenesis after deposition and the evolution of reservoir porosity of the Lower Jurassic reservoir in the Niudong area in-depth;

(3) to clarify the diagenetic stage of the target layer in the study area; and

(4) to analyze the control of primary sedimentary background and diagenesis on tight sandstone reservoirs. This result is crucial to the exploration and development of a similar low permeability reservoir in Qaidam Basin and similar reservoirs around the world.

2. Geological Setting

The Qaidam Basin, located in the northwest of the Qinghai-Tibet Plateau, is an inland intermountain basin developed after the Indosinian movement and a large Meso-Cenozoic petroliferous basin in northwest China [40,41]. The basin is bounded by the Qilian Mountain thrust fault zone in the north, the Kunlun Mountain strike-slip fault zone in the south, and the Altun strike-slip fault in the west, and covers a total area of 12×10^4 km^2, which has a special basin-mountain structural framework (Figure 1a) [42,43]. The formation and evolution of the Qaidam Basin is closely related to the activity of the Tethys-Himalayan tectonic domain. The compression and subduction of the Tethys oceanic crust to the paleo-Eurasian continent and the collision between the Indian and paleo-Asian plate caused a large uplift of the Qinghai-Tibet Plateau. The Qaidam Basin is formed under this complex geotectonic background and regional tectonic stress [44,45].

The Qaidam Basin can be divided into three first-order structural units: the western sag, the northern margin fault block, and the eastern sag [44,46]. The fault block of the northern margin of Qaidam Basin is located in the northwest of Qaidam Basin, which is approximately 440 km long from east to west and 65 km wide from north to south, covering an area of approximately 3000 km^2. The northern margin of Qaidam Basin consists of seven third-order structural units, namely: the Eboliang structural belt, Kunteyi fault depression, Lenghu structural belt, Saishiteng fault depression, Mahai-Dahonggou uplift, Yuka-Hongshan fault depression, and Delinha fault depression (Figure 1b).

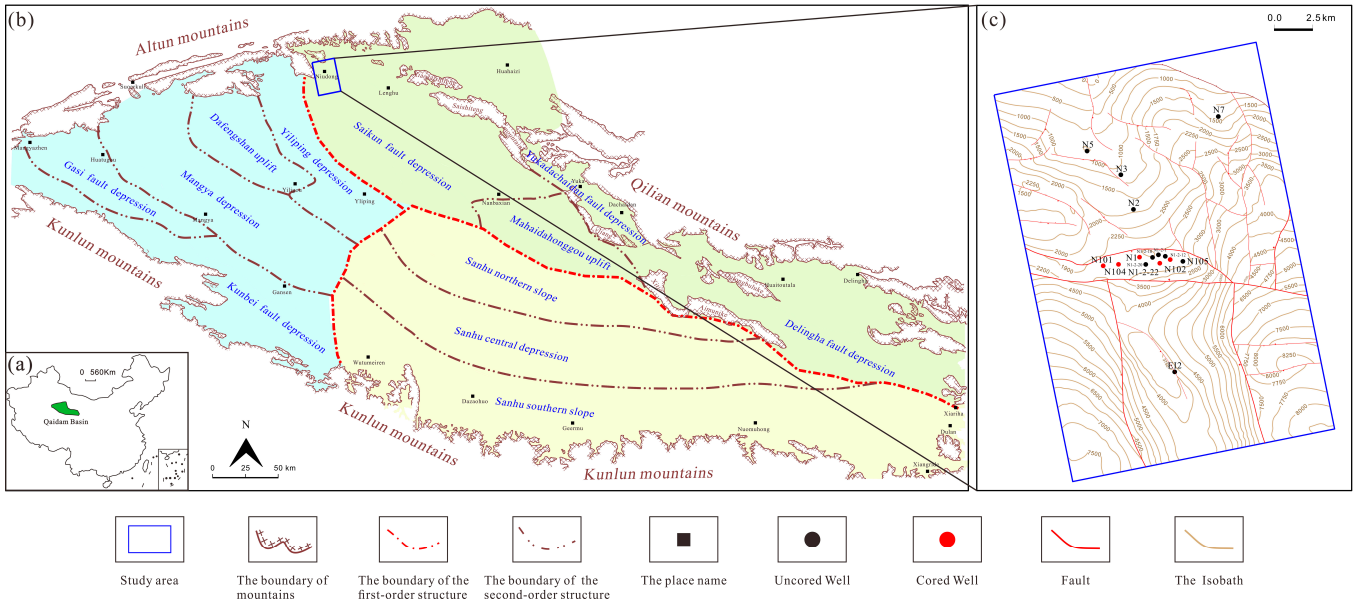

Figure 1. (**a**) Location of Qaidam Basin; (**b**) structure unit division in Qaidam Basin; (**c**) top structure contour map of the strata of the Lower Jurassic reservoir in Niudong.

Mesozoic-Cenozoic strata are developed in the northern margin of Qaidam Basin. The Mesozoic strata mainly developed in the Jurassic and Cretaceous periods. From old to new, the Jurassic period can be divided into Xiaomeigou Formation (J_{1x}), Dameigou Formation (J_{2d}), Caishiling Formation (J_3^{1c}), and Hongshuigou Formation (J_3^{2h}). The Quanyagou Formation (K_1) was mainly developed in the Cretaceous period. The old to new Cenozoic strata comprise the Lulehe Formation (E_{1+2}), Lower Member of Xiaganchaigou (E_3^1), Upper Member of Xiaganchaigou (E_3^2), Upper Ganchaigou Formation (N_1), Lower Youshashan Formation (N_2^1), Shangyoushashan Formation (N_2^2), Shizigou Formation (N_2^3), and the Qigequan Formation (Q_{1+2}) of Neogene (Figure 2) [40,47].

Niudong area is located in the eastern part of the front of Altun Mountain in the western part of the northern margin of Qaidam Basin, with the Kunteyi sag in the east and the Eboliang I structure in the south (Figure 1b). The Niudong area is an inherited paleo-uplift formed in the late Yanshanian period, and is generally characterized by a large nose uplift structure dipping into the basin in front of the mountain with frequent fractures; the exploration area is close to 500 km^2 (Figure 1b,c) [36]. The discovery of the Niudong gas field proves that the Niudong area has great exploration potential [39]. The Niudong gas reservoir mainly developed in the Jurassic strata, and the lithology of the Jurassic strata mainly comprises gray-white conglomerate, sand conglomerate, a large set of thick dark mudstone, and coal-bearing source rocks. Jurassic strata in this area is also one of the important exploration targets in the northern margin of Qaidam Basin [39].

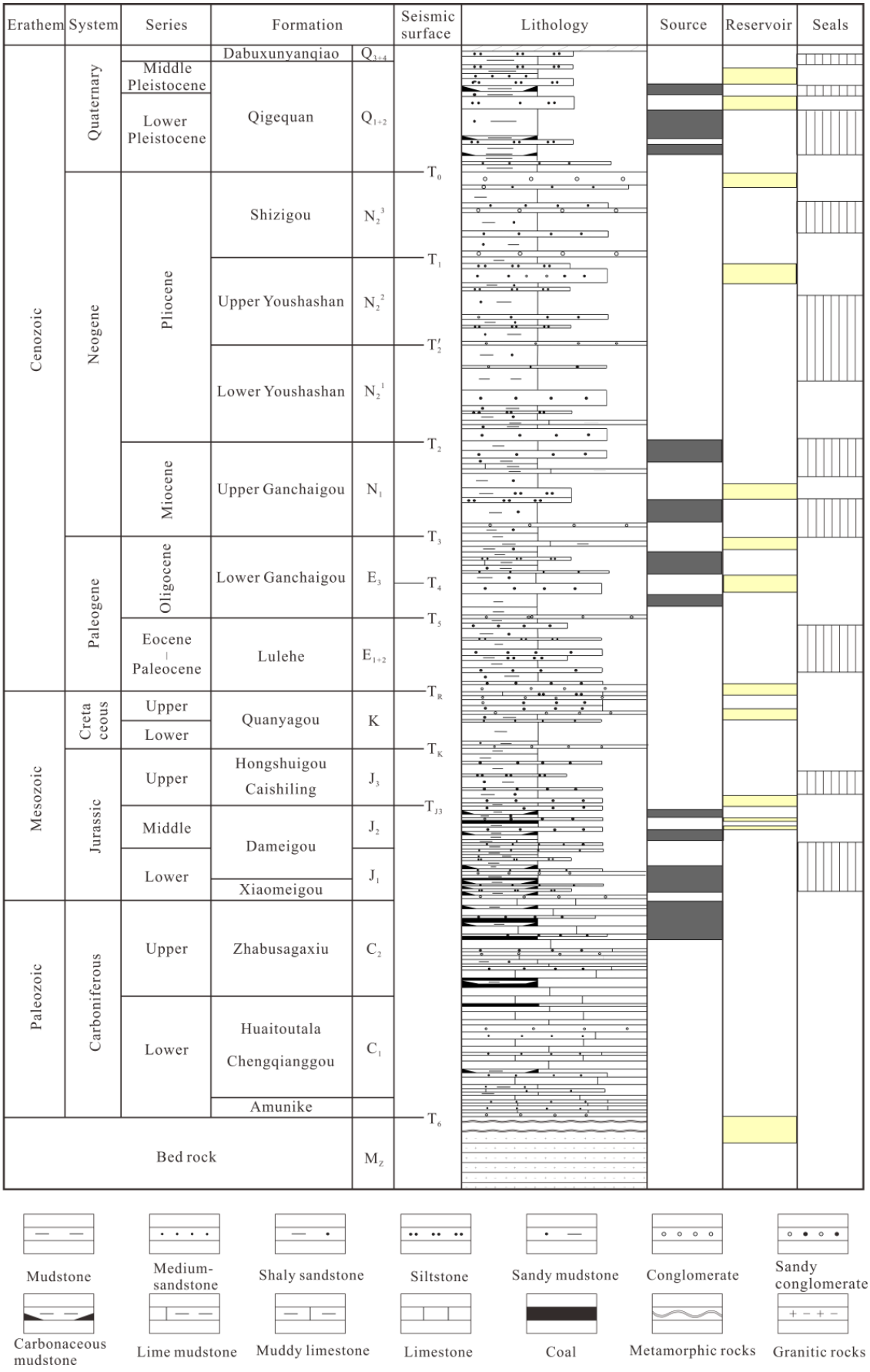

Figure 2. Stratigraphy column of the Qaidam Basin.

3. Samples and Methods

A total of 293 core samples were obtained from six exploration wells of the Lower Jurassic reservoirs in the Niudong area in the northern margin of Qaidam Basin, and were used in the casting thin section, grain size examination, scanning electron microscopy, helium porosity and permeability, X-ray diffraction, carbon and oxygen stable isotope, and vitrinite reflectance (Ro) experiments to analyze the microscopic pore system, sedimentary structure, diagenetic characteristics, and petrological and physical properties of Lower Jurassic reservoirs in the Niudong area.

3.1. Casting Section

According to the method proposed by Dickson (1966) [48], 53 samples were selected from six wells to prepare casting thin sections, which were used to observe the type, characteristics, and distribution of pores as well as the relationship between skeleton particles. All slices were vacuum impregnated with blue-stained epoxy resin and dyed with alizarin red and potassium ferricyanide to distinguish carbonate minerals, with calcite being stained pink and ferroan calcite dark red to purple. The thin slices were observed using the ZEISS imager (China University of Geosciences, Beijing, China). An A2 polarizing microscope (China University of Geosciences, Beijing, China) was used, and 350 points were counted on each thin section for the analysis of their petrological and mineralogical characteristics.

3.2. Granularity Analysis

The particle size analysis data of 126 samples were collected from the Qinghai Oilfield Research Institute. The particle size was measured using the Mastersizer 2000 laser particle size analyzer, and the separation coefficient, average particle size, and median particle size were determined according to the standard chart proposed by Trask (1932).

3.3. Scanning Electron Microscope

Scanning electron microscopy can be used to determine the types and morphology of intergranular cements and the authigenic clay minerals in samples, and to simultaneously observe the characteristics of micropores and diagenesis. For the preparation of gold-plated slices, 68 sandstone samples from six wells were selected and observed using the ZEISSEVO-18 scanning electron microscope (Experimental Research Center of Unconventional Technology Research institute of CNOOC, Beijing, China).

3.4. X-ray Diffraction Analysis

To accurately determine the mineral content, the clay mineral type and ratio of the smectite layer in illite/smectite mixed layer, 80 samples from five wells were ground using an agate bowl and grinding machine. According to the SY/T5163-2010 standard, the whole rock and clay mineral compositions of the samples were analyzed using the Empyrean sharp shadow X-ray diffractometer made by Panaco Company in the Netherlands (China University of Geosciences, Beijing, China).

3.5. Helium Porosity

To evaluate the reservoir space (porosity) and percolation capacity (permeability) of the reservoir 285 core samples with diameters of 2.5 cm were drilled from six coring wells to measure porosity and permeability. Porosity and permeability were measured using the UltraPore-400 porosity tester (Experimental research center of Wuxi research institute of petroleum geology of SINOPEC, Wuxi, China) and DX-07G permeability tester (Experimental research center of Wuxi research institute of petroleum geology of SINOPEC, Wuxi, China), respectively.

3.6. Maturity of Organic Matter

Vitrinite reflectance is an effective parameter for evaluating the thermal maturity of hydrocarbon source rocks, which is closely related to the diagenetic stage [49]. Therefore, vitrinite reflectance values of 14 mudstone samples from three wells were measured. The MPM600 microphotometer (Experimental research center of Wuxi research institute of petroleum geology of SINOPEC, Wuxi, China) was used to measure the random average Ro of these samples and each sample was measured more than ten times. The reflectivity of each sample was calculated by averaging the histogram of the data.

3.7. Carbon and Oxygen Stable Isotope Analysis

Twelve core samples with developed carbonate cements were selected to measure carbon and oxygen stable isotopes. These core samples were crushed below 200 mesh and then reacted fully with 100% H_3PO_4 at a constant temperature. In this process, CO_2 gas was produced, which was collected and purified to measure stable carbon and oxygen isotopes using a MAT253 stable isotope mass spectrometer (Experimental research center of Wuxi research institute of petroleum geology of SINOPEC, Wuxi, China). The results of the carbon and oxygen isotope analyses are presented using standard δ notation according to the V-PDB (Vienna PeeDee Belemnite) standard and the analytical precision are ±0.06‰ for $\delta^{13}C$ and ±0.08‰ for $\delta^{18}O$ values.

4. Results

Based on the above experiments, some understanding about the Lower Jurassic reservoir in the Niudong area was obtained. This paper will introduce the understanding and results from petrological characteristics, reservoir physical properties, reservoir pore types and pore throat characteristics, diagenesis characteristics, and organic matter maturity.

4.1. Reservoir Petrological Characteristics

The Jurassic strata in the Niudong area mainly developed in the early Jurassic strata, and the sedimentary background comprises of fan delta-lacustrine deposits. Core observation and thin section identification showed that the sandstone types in the study area mainly comprised feldspathic litharenite, lithic arkose, followed by arkose, and litharenite (Figure 3). Quartz content in sandstone ranged from 11.0% to 52.0% (average of 27.1%); feldspar content ranged from 8.8% to 64.6% (average of 32.5%); and the rock fragments content from 4.2% to 69.1% (average of 40.4%). The main types of rock fragments were metamorphic rock debris, followed by igneous rock debris and a low volume of sedimentary rock debris. The main contact between particles was point contact, followed by point-line contact. The sorting property of rocks mainly ranges from medium to poor, and the roundness is mainly subangular, followed by subangular-subrounded. Pore cementation was the main type of cementation, and the mud content was low, with an average of 8.1%.

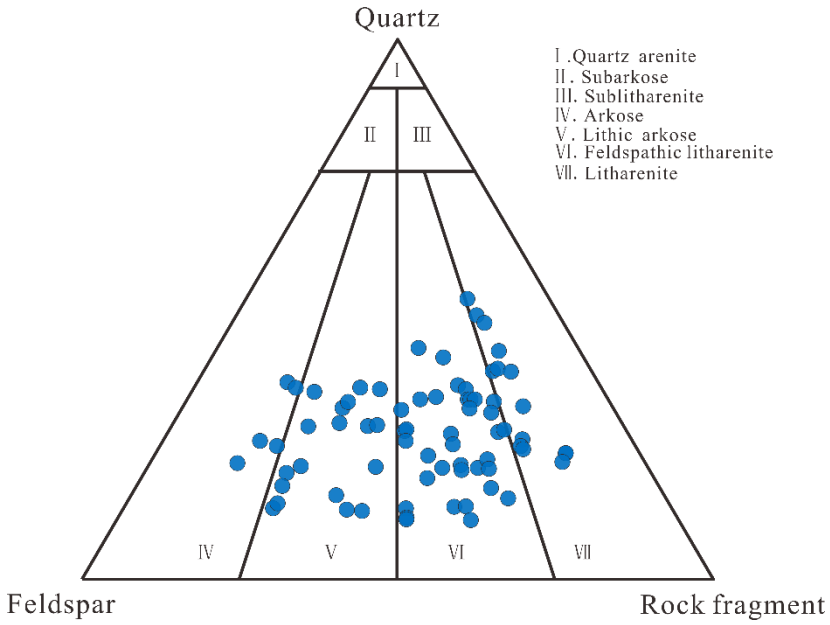

Figure 3. Ternary diagram of detrital compositions of the sandstones in the Lower Jurassic reservoir in Niudong based on the Folk (1980) sandstone classification [50].

4.2. Pore Types and Pore Throat Characteristics

The results of casting thin section and scanning electron microscopy showed that secondary pores were the main pore types in the Lower Jurassic reservoir in Niudong, followed by fractures, and a small amount of residual intergranular pores. The secondary pores included intergranular and intragranular pores. The intergranular pores were mainly distributed on the edge of soluble materials such as feldspar, and were bay or irregularly shaped (Figure 4a,b). The intragranular pores mainly occurred in the interior of feldspar or debris, and were irregularly shaped (Figure 4a–c). Fractures are mainly caused by compaction and various tectonic stresses, which are beneficial to acidic or alkaline fluids permeating into particles, causing the dissolution of particles and the formation of dissolution fractures (Figure 4a,e,f). Microfractures are commonly developed in tight sandstones in the study area and can be divided into three types: transgranular fractures, intragranular fractures, and the fracture around the grains (Figure 4e,f).

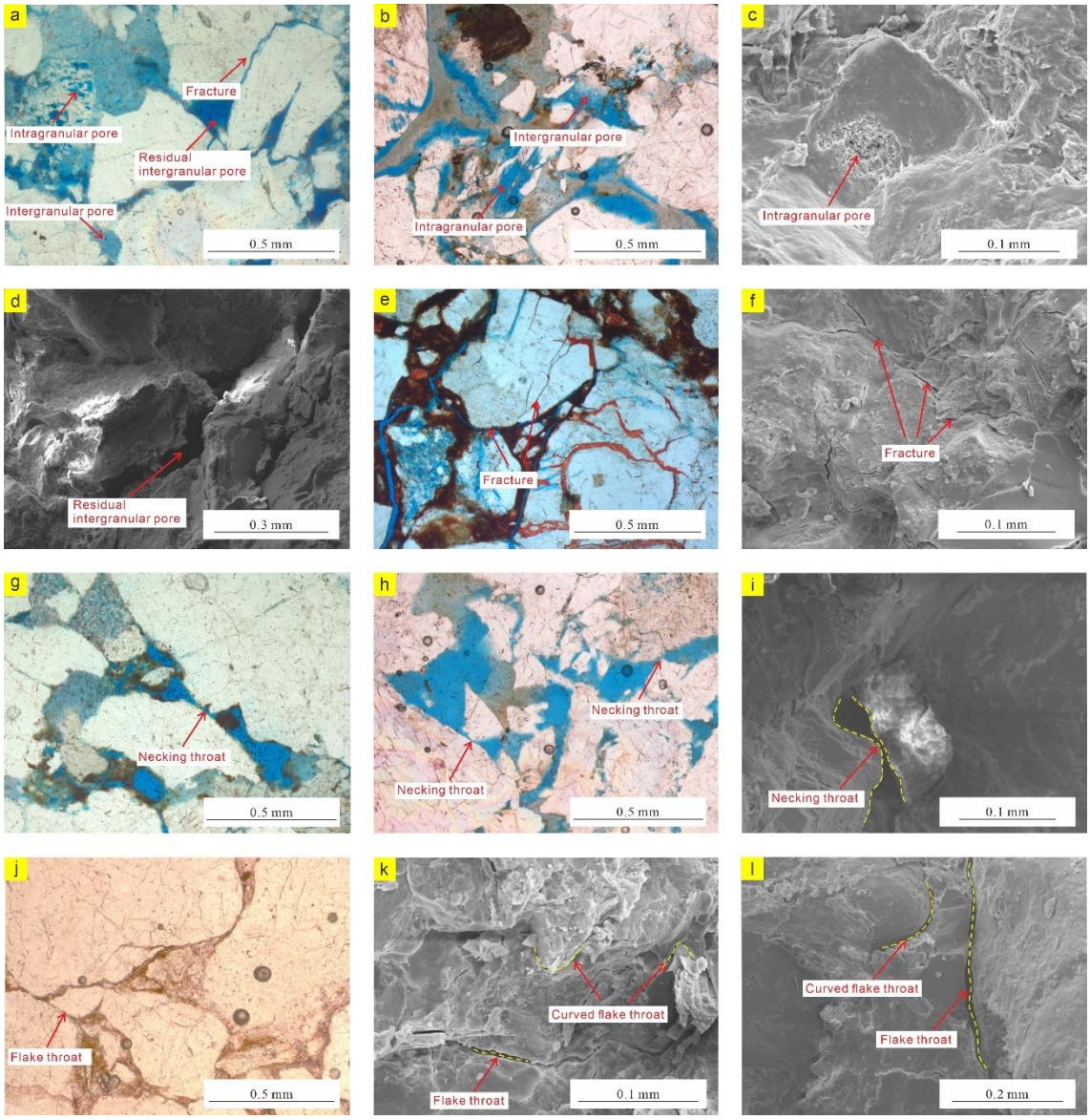

Figure 4. Pore types and pore-throat characteristics in the Niudong area, northern margin of Qaidam Basin: (**a**) N1, 2225.0 m, intragranular pore, intergranular pore, fracture, residual intergranular pore; (**b**) N102, 2120.5 m, intragranular pore, intergranular pore; (**c**) N102, 2113.6 m, intragranular pore; (**d**) N102, 2120.5 m, residual intergranular pore; (**e**) N104, 2054.8 m, fracture; (**f**) N1-2-22, 2149.6 m, fracture; (**g**) N1, 2226.0 m, necking throat; (**h**) N102, 2114.7 m, necking throat; (**i**) N101, 3621.1 m, necking throat; (**j**) N101, 2120.5 m, flake throat; (**k**) N1-2-22, 2149.4 m, flake throat, curved flake throat; (**l**) N101, 3623.2 m, flake throat, curved flake throat.

As a bridge between pores, the shape and size of the throat play an influential role in fluid migration and permeability in the reservoir [51]. According to the analysis results of the casting thin section and scanning electron microscopy, the throats of the lower Jurassic reservoir in Niudong is mainly divided into three types:

(a) Necking throat: a part of the shrinkage part between particles due to the close contact of particle compaction, which features a pore radius larger than the throat radius. Although the pore is large, the seepage capacity is poor, and this kind of throat is relatively developed in the study area (Figure 4g–i);

(b) Flake throat: mostly found in sandstone with linear or concave–convex contact [51]. It features small pores and a fine throat, and is also common in the study area (Figure 4j–l);

(c) Curved flake throat: small, curved, and rough, and is easily blocked (Figure 4k,l). It is generally formed under strong compaction, which causes the inlaid particles to come into contact with each other, thus easily forming a curved throat.

4.3. Porosity and Permeability

The porosity and permeability of 285 samples from six wells in the Niudong area were measured, and the results show that the main porosity ranged from 8.0% to 10.0%, the maximum value was 19.5%, the minimum value was 0.01%, and the average was 9.9% (Figure 5a). The main permeability varied from 0.5 to 5.0 mD, the maximum value was 32.4 mD, the minimum value was 0.01 mD, and the average was 3.8 mD, which exhibited a typical low permeability sandstone reservoir (Figure 5b). In addition, a strong linear relationship was observed between porosity and permeability (Figure 5c) (R^2 = 0.6643).

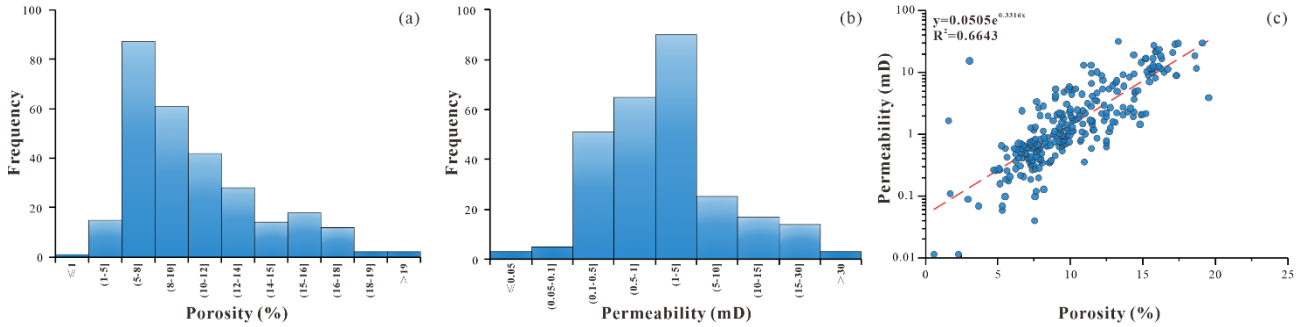

Figure 5. Physical properties of sandstone reservoirs in the Lower Jurassic in the Niudong area, northern margin of Qaidam Basin: (**a**) distribution of porosity; (**b**) distribution of permeability; (**c**) relationship between porosity and permeability.

4.4. Diagenesis

By analyzing the thin sections, casting thin sections, and scanning electron microscopy of six coring wells, the types of diagenesis in the study area were observed to mainly include compaction, cementation, and dissolution among others. Compaction was found to have the greatest influence on reservoir physical properties.

4.4.1. Compaction

The present buried depth of the Lower Jurassic reservoir in the Niudong area is 1400–4800 m (average of 2200 m), with a large depth span. Compaction is the main factor affecting the deterioration of physical properties of Lower Jurassic reservoirs in the study area. According to the observation of thin sections, the compaction can be divided into the following four types in detail:

(a) Particles in close proximity with each other. Most of the particles are in point-line contact. Where the compaction is strong, line–concave–convex contact is observed and pressure solution occurs (Figure 6a–c);

(b) Particles follow a directional pattern. Under the action of overlying strata pressure, the particles are oriented, which is mainly characterized by the directional arrangement of flake minerals such as mica (Figure 6d);

(c) Plastic particles are deformed by extrusion. Where the compaction is strong, plastic materials such as mica can be bent or broken (Figure 6e);

(d) Rigid particles are crushed by extrusion. As burial depth increases, the compaction gradually increases, and certain rigid particles such as quartz and feldspar are evidently extruded and broken, forming micro-fractures (Figure 6f).

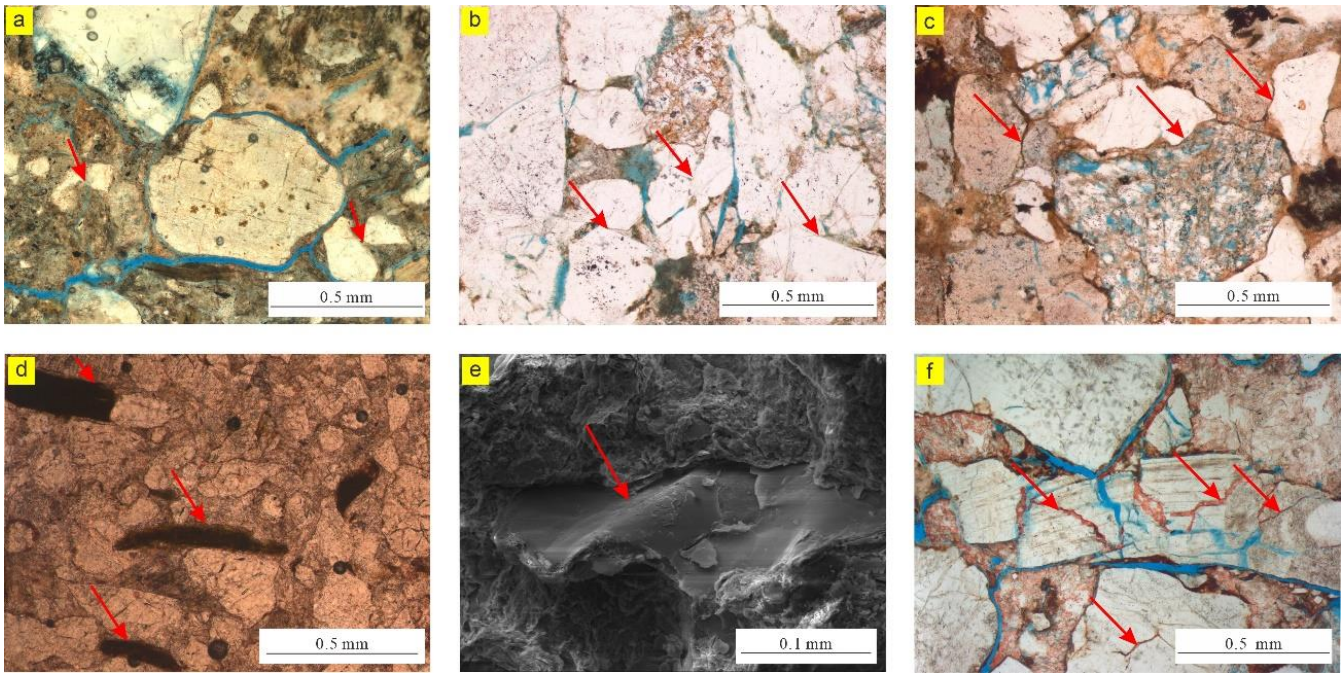

Figure 6. Characteristics of compaction in the Lower Jurassic reservoir in the Niudong area: (**a**) N1-2-22, 2146.2 m, point contact; (**b**) N102. 2112.0 m, point-line contact; (**c**) N102, 2066.5 m, line contact; (**d**) N104, 2366.1 m, directional arrangement of mica; (**e**) N102, 2067.0 m, mica extrusion deformation; (**f**) N104, 2052.4 m, fracture.

4.4.2. Cement

Cementation refers to the precipitation of minerals from pore solution and the consolidation of loose rocks, which is one of the important factors contributing to reducing the porosity and permeability of sandstone reservoirs [51]. In contrast to compaction, cementation reduces reservoir physical properties mainly by reducing the connectivity of the pore throat. Cementation can occur at all diagenetic stages, and the forms and types of the cements vary according to the different conditions of water media in the diagenetic environment such as PH value and trace elements [52]. The cementation of Lower Jurassic reservoirs in the Niudong area is strong, and the types of cementation mainly include carbonate cementation, siliceous cementation, and clay mineral cementation.

Carbonate Cement

The carbonate cement in the Lower Jurassic reservoir in this study area mainly comprises calcite, followed by a small amount of iron-bearing calcite. Three different kinds of carbonate cements at different stages were identified via thin section analysis: (a) In the early stage, the compaction was weak, the contact between particles was mainly in the floating state, the carbonate cement mainly comprised of micrite calcite, calcite appeared in basal cementation, and calcite content was relatively low (Figure 7a); (b) In the middle stage, calcite cementation was predominant in the carbonate cement, which appeared as pore cementation, and was often intercrystalline filled between the skeleton particles (Figure 7b); and (c) In the later stage, a small amount of iron-bearing calcite was observed to fill the intergranular pores.

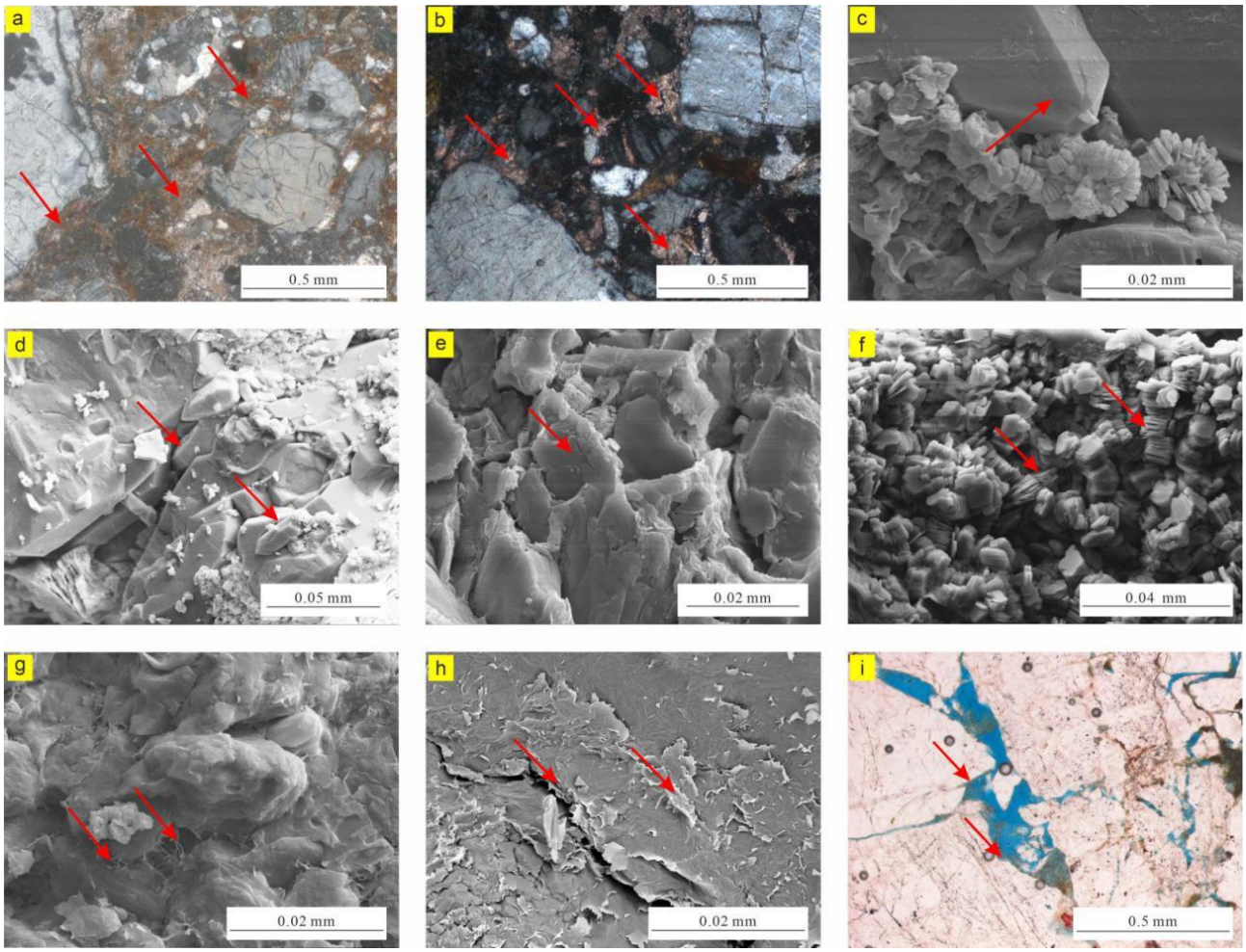

Figure 7. Characteristics of cementation in Lower Jurassic reservoir in the Niudong area: (**a**) N101, 3622.1 m, calcite with basal cement; (**b**) N104, 2364.9 m, calcite with porous cementation; (**c**) N1-2-1, 1975.2 m, quartz overgrowth in III grade; (**d**) N102, 2113.8 m, quartz overgrowth degree of grade III; (**e**) N1-2-1, 1966.9 m, kaolinite on particle surface; (**f**) N102, 2020.5 m, page-shaped kaolinite filling intergranular pores; (**g**) N106, 2836.5 m, filaments of illite; (**h**) N104, 2369.7 m, illite/smectite mixed layer on particle surface; (**i**) N102, 2117.2 m, chlorite films.

Quartz Overgrowth

The siliceous cementation in the study area is mainly characterized by quartz overgrowth (Figure 7c,d), and the main degree of enlargement was grade II–III. The quartz overgrowth formed along the edge of the quartz, where it occupied intergranular pores and reduced pore space. At the same time, the quartz overgrowth improves the compression resistance of the reservoir and can alleviate the destructive effect of compaction on the reservoir [51].

Authigenic Clay Minerals

The composition, morphology, and occurrence of clay minerals are of great significance to the physical properties of tight reservoir [53]. The scanning electron microscopy and X-ray diffraction analysis results showed that the authigenic clay minerals in the study area included kaolinite, illite/smectite mixed layer, illite and chlorite, among which kaolinite was the most developed, followed by illite and the illite/smectite mixed layer. In addition, chlorite content was relatively low (Figure 8). Moreover, from the wells N1 to EI2, during the advancement from piedmont to lake, the kaolinite content decreased gradually, whereas the illite/smectite mixed layer content increased gradually.

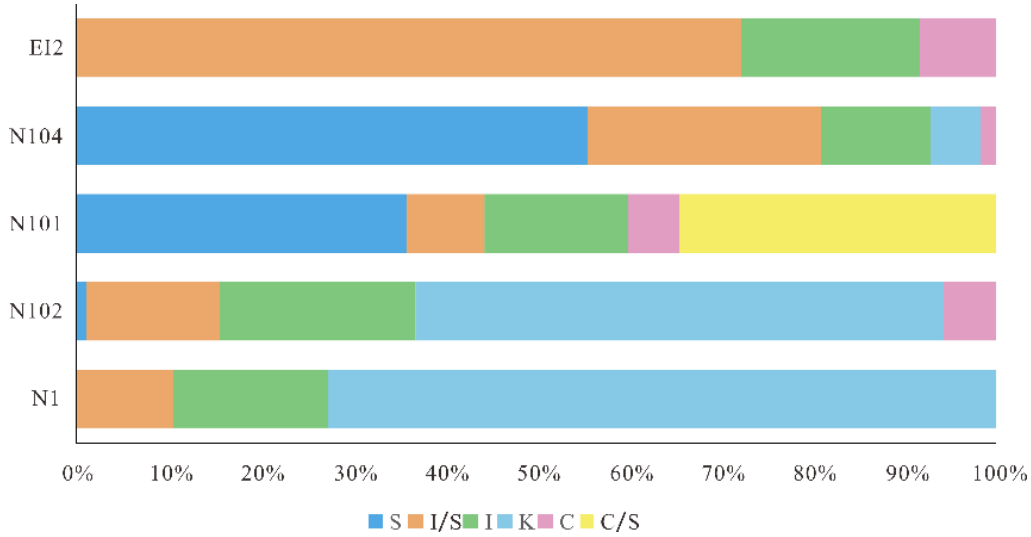

Figure 8. X-ray diffraction analysis of authigenic clay minerals in Lower Jurassic reservoir in Niudong, northern margin of Qaidam Basin.

Kaolinite

According to the particle morphology and crystallization degree, two types of kaolinite were identified in the study area. (a) Kaolinite adsorbed on the particle surfaces in flakes or worm shapes, with an irregular edge caused by dissolution. This kind of kaolinite is generally formed in the early diagenetic stage and is caused by the dissolution of plagioclase and potassium feldspar under the action of organic acid (Figure 7e). (b) The morphology of kaolinite was well developed. The single crystal was pseudo-hexagonal plate-like, and the aggregates filled the intergranular pores or feldspar dissolved pores in the form of booklet-like (Figure 7c,f). This kind of kaolinite is generally formed in the late diagenetic stage and is precipitated directly in the pore solution or gradually evolved from the early kaolinite with a smaller crystal shape [54]. The second type of kaolinite is widely developed in the study area.

Illite

Illite is often formed in the late diagenetic stage. Under the scanning electron microscope, the monomer was ribbon-like, and the aggregate was honeycomb-like or filamentous, which can block the intergranular pores and secondary dissolved pores to a certain extent (Figure 7g).

Illite/Smectite Mixed Layer

The morphology of the illite/smectite mixed layer was between illite and smectite, which is the intermediate product of the transformation from smectite to illite or chlorite [53,55]. Scanning electron microscopy showed that the illite/smectite mixed layer was filled in intergranular pores and secondary dissolved pores in the form of hair or curly flakes. At the same time, as the hair-like or flake-like morphology of the illite/smectite mixed layer can segment the pore space, the connectivity of the pore-throat was attenuated (Figure 7h)

Chlorite

Chlorite in the study area is mainly produced in the form of pore films or pore linings growing vertically along the surface of the debris particles. This appeared to be rose-shaped or as a honeycomb composed of leaves under the scanning electron microscope (Figure 7i).

4.4.3. Dissolution

Dissolution plays an important role in the improvement of physical properties of low permeability sandstone reservoirs [4,30,56]. The Lower Jurassic reservoir in the Niudong

area exhibits five types of strong dissolution: (a) The insides of the particles are dissolved by acidic fluid such as the dissolution of feldspar, and often form intragranular solution pores in the shape of spots or honeycombs (Figure 9a,b); (b) the particles are strongly dissolved and the whole particles are dissolved to form moldic pores (Figure 9c); (c) feldspar particles dissolve along their cleavage crack or fractures, forming intragranular pores, which can effectively improve reservoir connectivity (Figure 9d,e); (d) irregular dissolution occurs at the edges of soluble particles such as feldspar and lithic debris, forming intergranular pores (Figure 9a,b); and (e) a small amount of dissolution occurs in interstitial materials such as calcite, forming interstitial dissolution pores and intergranular pores (Figure 9f).

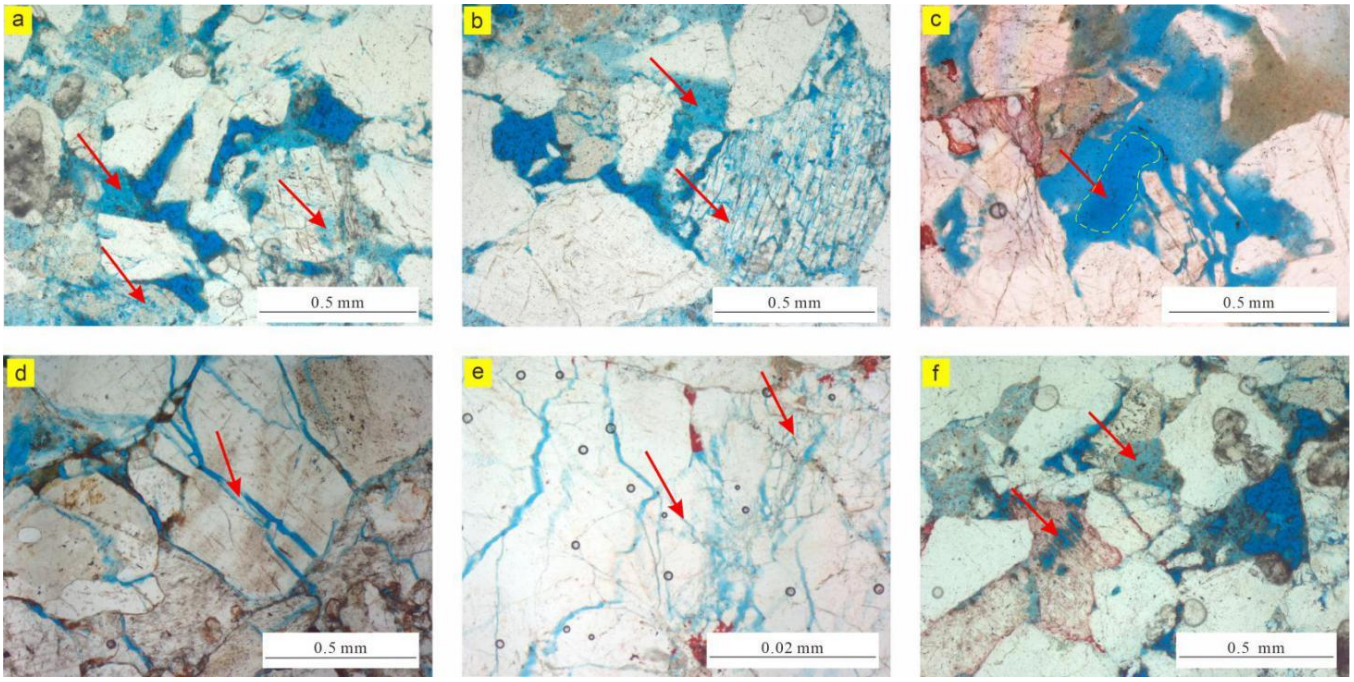

Figure 9. Characteristics of dissolution in Lower Jurassic reservoir in the Niudong area: (**a**) N1, 2232.5 m, intergranular dissolution pores in feldspar, intragranular dissolution pores; (**b**) N1, 2225.6 m, intragranular dissolution pores, intergranular dissolution pores; (**c**) N102, 2119.5 m, the whole feldspar is dissolved to form moldic pore; (**d**) N104, 2052.4 m, feldspar dissolution along the cleavage crack or fracture; (**e**) N106, 2814.0 m, feldspar dissolution along the cleavage crack or fracture; (**f**) N1, 2232.5 m, debris is dissolved, calcite is dissolved.

4.5. Maturity of Organic Matter

The thermal maturity index of organic matter can provide information on the paleo-geotemperature that the organic matter was subjected to and used to identify the diagenetic stage. Vitrinite reflectance (Ro) was used in this paper. The change in vitrinite reflectance (Ro) was mainly related to temperature, and the temperature information of the reaction was irreversible, making it a suitable basis for dividing diagenetic stages in the study of diagenesis [57]. The vitrinite reflectance (Ro) of organic matter in the mudstone of the Lower Jurassic reservoir in the Niudong area ranged between 0.876 and 1.379 (Table 1), with an average of 1.143%.

Table 1. Vitrinite reflectance of mudstone kerogen in the Lower Jurassic reservoir in Niudong, northern margin of Qaidam Basin.

Well	Depth(m)	Lithology	Sample	Ro, ran%
N2	2038	Grey black mudstone	kerogen	1.379
N2	2210	Black carbonaceous mudstone	kerogen	0.876
N2	2159	Coal	kerogen	1.175
		Average		1.143

4.6. Carbon and Oxygen Stable Isotope

The carbon and oxygen isotope measurement results of 12 samples showed that the $\delta^{13}C$ values (V-PDB) in the study area ranged from −13.8‰ to −3.1‰, with an average of −9.6‰; and the $\delta^{18}O$ value (V-PDB) ranged from −19.3‰ to −12.4‰, with an average of −15.0‰ (Table 2).

Table 2. Carbon and oxygen isotope data of carbonate cements of the Lower Jurassic reservoir in Niudong, northern margin of Qaidam Basin.

Well	Depth (m)	$\delta^{13}C_{PDB}$‰	$\delta^{18}O_{PDB}$‰
N1	2227.17	−10.31	−12.37
N1	2227.90	−9.86	−12.87
N1	2228.72	−10.56	−14.39
N1	2231.53	−9.68	−13.78
N1	2232.17	−9.51	−15.96
N104	2366.50	−5.57	−14.94
N104	2367.30	−5.69	−13.43
N104	2369.70	−3.10	−13.81
EI2	4644.93	−13.79	−16.47
EI2	4647.90	−12.96	−15.98
EI2	4837.75	−12.15	−16.37
EI2	4839.84	−12.32	−19.34
Average		−9.63	−14.98

5. Discussion

The diagenetic mechanism of porosity evolution is of great significance to the low permeability sandstone reservoir. Therefore, it is necessary to quantitatively analyze the pore evolution process of the reservoir, which is still a gap in the study area. Besides, previous studies have only qualitatively analyzed the controlling factors of the Lower Jurassic reservoirs in the Niudong area, and the controlling effects of sedimentation and fracture have not been discussed [39]. Therefore, based on an understanding of the study area, the evolution of reservoir porosity, the diagenesis stages, and the controlling factors of reservoirs can be further discussed in this paper.

5.1. The Evolution of Reservoir Porosity

Porosity is one of the important parameters of determining the quality of the reservoir, which determines the storage capacity of oil and gas. For low permeability sandstone reservoirs, whose permeability is low, porosity becomes a key parameter of determining the industrial capacity of the reservoir. The present porosity is the result of a series of diagenetic reformation based on the preservation of primary pores; therefore, quantitative analysis of the law of porosity evolution in the diagenetic process of low permeability sandstone reservoir is crucial.

5.1.1. Initial Porosity of Unconsolidated Sandstone

The recovery of porosity evolution requires the initial porosity of unconsolidated sandstone. The quantitative model of porosity evolution proposed by geologists Beard and

Weyl in the 1970s is used to calculate the initial porosity of unconsolidated sandstone [25]. The formulas are expressed as follows:

$$\Phi_1 = 20.91 + 22.90/S_d \quad (1)$$

$$S_d = [Q_{25}/Q_{75}]^{1/2} \quad (2)$$

In Equation (1), Φ_1 is the initial porosity of unconsolidated sandstone, %; in Equation (2), S_d is the sorting coefficient; and Q_{25} and Q_{75} respectively correspond to the diameters of particles equating to 25% and 75% on the grain size accumulation curve respectively, mm.

According to the thin section statistical analysis and grain size data, the sorting coefficient of sandstone in the Lower Jurassic reservoir in the Niudong area ranged from 1.9–3.0, with an average of 2.3. According to the formula above, the initial porosity (Φ_1) of unconsolidated sandstone was 28.6–33.0%. The average value was 31.2% (Table 3), which was significantly lower than the conventional view of 40.0%.

5.1.2. Porosity of Compacted Sandstone

After the sediment enters the burial period, the loss of primary pores is mainly attributed to compaction [21]. Because of compaction, some of the primary pores are lost directly, and the rest are cemented. Therefore, the porosity of the remaining sandstone after compaction can be calculated according to the relationship between the residual primary intergranular pores, cement content, dissolution pore surface porosity, and measured physical property analysis pores. The formula is expressed as follows:

$$\Phi_2 = W + \frac{P_1}{P_2} \times P_3 \quad (3)$$

In Equation (3), Φ_2 is the porosity of residual sandstone after compaction, %; W is the percentage content of cement, %; P_1 is the primary intergranular porosity, %; P_2 is the total area porosity, %; and P_3 is the measured porosity of the physical property, %.

$$\text{Porosity lost by Compaction} = \Phi_1 - \Phi_2 \quad (4)$$

$$\text{Compaction porosity loss rate} = \frac{(\Phi_1 - \Phi_2)}{\Phi_1} \times 100\% \quad (5)$$

According to the calculation and analysis of casting thin section data (Table 3), the primary intergranular pore surface porosity (P_1) was 0.0–6.0%, with an average of 1.2%; the total surface porosity (P_2) was 0.2–15.0%, with an average of 5.0%; and the measured physical property analysis porosity (P_3) was 4.3–18.7%, with an average of 9.8%. The cement content (W) was 2.0–21.0%, with an average of 8.0%.

According to the formula above, the porosity (Φ_2) of the remaining sandstone after compaction was 1.8–21.0%, with an average of 9.7% (Table 3).

Table 3. Parameters for quantitative calculation of pore recovery in the Niudong area.

Well	Core Porosity	Cementation	Primary Pore %	Secondary Pore %	Fracture %	Thin Section Porosity %	Sorting S_d	Unconsolidated Porosity Φ_1	Porosity after Compaction Φ_2	Porosity after Cementation Φ_3	Second Pore Porosity in Thin Sections Φ_4	Fracture Porosity in Thin Sections Φ_5
N102	4.6~18.7 10.4(18)	4.0~15.0 10.5(18)	0.0~6.0 3.5(18)	1.0~6.0 2.6(18)	0.0~1.0 0.1(18)	2.0~10.0 6.2(18)	1.9~2.6 2.1(18)	29.9~33.0 31.9(18)	6.0~20.6 15.4(18)	0.0~8.2 4.9(18)	1.~18.7 5.4(18)	0.0~1.2 0.1(18)
N1-2-22	12.2~16.6 14.8(3)	2.0~17.0 7.7(3)	0.0 0.0(3)	2.0~5.00 4.0(3)	0.0 0.0(3)	2.0~5.0 4.0(3)	2.0~2.6 2.4(3)	29.7~32.1 30.5(3)	2.0~17.0 7.7(3)	0.0 0.0(3)	12.2~16.6 14.8(3)	0.0 0.0(3)
N1	4.5~16.3 10.9(8)	2.0~15.0 6.6(8)	0.0 0.0(8)	3.0~15.0 10.3(8)	0.0 0.0(8)	3.0~15.0 10.3(8)	2.7 2.7(8)	29.5 29.5(8)	2.0~15.0 6.6(8)	0.0 0.0(8)	4.5~16.3 10.9(8)	0.0 0.0(8)
N104	7.3~12.4 10.2(10)	4.0~21.0 8.5(10)	0.0 0.0(10)	0.0~1.0 0.1(10)	1.0~5.0 3.4(10)	1.0~5.0 3.5(10)	2.0~3.0 2.2(10)	28.6~32.5 31.6(10)	4.0~21.0 8.5(10)	0.0 0.0(10)	0.0~2.4 0.2(10)	7.3~12.4 9.9(10)
N101	4.7~14.4 8.0(9)	3.0~9.0 5.7(9)	0.0 0.0(9)	0.0 0.0(9)	1.0~3.0 2.2(9)	1.0~3.0 2.2(9)	2.0~2.2 2.2(9)	31.2~32.1 31.5(9)	3.0~9.0 5.7(9)	0.0 0.0(9)	0.0 0.0(9)	4.7~14.4 8.0(9)
EI2	4.3~7.1 5.4(5)	1.8~7.0 4.5(5)	0.0~0.1 0.0(5)	0.1~1.6 0.6(5)	0.0~0.1 0.1(5)	0.2~1.8 0.7(5)	2.3~2.7 2.6(5)	29.3~3.1 30.0(5)	1.8~7.0 4.6(5)	0.0~0.4 0.1(5)	2.1~6.5 4.7(5)	0.0~2.1 0.6(5)
Total	4.3~18.7 9.8	2.0~21.0 8.0	0.0~6.0 1.3	0.0~15.0 2.7	0.0~5.0 1.1	0.2~15.0 5.0	1.9~3.0 2.3	28.6~33.0 31.2	1.8~21.0 9.7	0.0~8.2 1.7	0.0~18.7 4.8	0.0~14.4 3.3

5.1.3. Porosity of Sandstone after Cementation

Based on compaction, cementation such as clay minerals, carbonate minerals, and quartz overgrowth will cause further loss of primary pores. The porosity of sandstone after compaction and cementation (Φ_3) is the porosity of the final intergranular pores, as expressed below:

$$\Phi_3 = \frac{P_1}{P_2} \times P_3 \quad (6)$$

$$\text{Loss of porosity by cementation} = \Phi_2 - \Phi_3 \quad (7)$$

$$\text{Cementation porosity loss rate} = \frac{\Phi_2 - \Phi_3}{\Phi_1} \times 100\% \quad (8)$$

After cementation, the remaining porosity Φ_3 of Lower Jurassic reservoirs in the Niudong area was 0.0–8.2% (av. 1.7%).

5.1.4. Secondary Porosity

Secondary porosity (Φ_4) refers to the part of reservoir space occupied by dissolved pores in the total reservoir space [33], and the calculation formula is:

$$\Phi_4 = \frac{P_4}{P_2} \times P_3 \quad (9)$$

where P_4 is the dissolution pores in the thin section porosity, %.

According to the calculation and analysis of the casting thin sections, the porosity (P_4) of dissolved pores was 0.0–15.0%, with an average value of 2.7%. Therefore, the secondary porosity (Φ_4) of Lower Jurassic reservoirs in the Niudong area was 0.0–18.7%, with an average of 4.8%.

5.1.5. Fractures

The porosity increased by fractures (Φ_5) refers to the part of the reservoir space occupied by fractures in the total reservoir space,

$$\Phi_5 = \frac{P_5}{P_2} \times P_3 \quad (10)$$

where P_5 is the thin section porosity of the fractures, %.

According to Equation (10), the thin section porosity of the fractures (P_5) was calculated as 0.0–5.0% with an average of 1.06%. Therefore, the porosity increased by fractures (Φ_5) in the Lower Jurassic reservoir in the Niudong area was 0.0–14.4%, with an average of 3.3%.

5.1.6. Pore Evolution Analysis

As seen in Table 3, the initial porosity in the Niudong area was 31.2%, and the loss of porosity in the compaction process was 21.5%. After compaction, the remaining intergranular porosity was 9.7%, and the porosity loss rate caused by compaction was 69.0%. The porosity loss rate caused by clay mineral cementation, carbonate cementation, and quartz overgrowth was 25.7%, and the porosity after cementation was 1.7%. The dissolution intensity in the Niudong area was strong, and the later soluble materials such as feldspars, rock fragments, and carbonate cement contributed to 4.8% of the porosity. The increasing rate of porosity in the dissolution process was 15.5%. The current porosity was 6.5%, and the porosity of the physical property analysis was 9.8%. According to the analysis above, the evolution model of diagenesis for physical porosity was obtained (Figure 10).

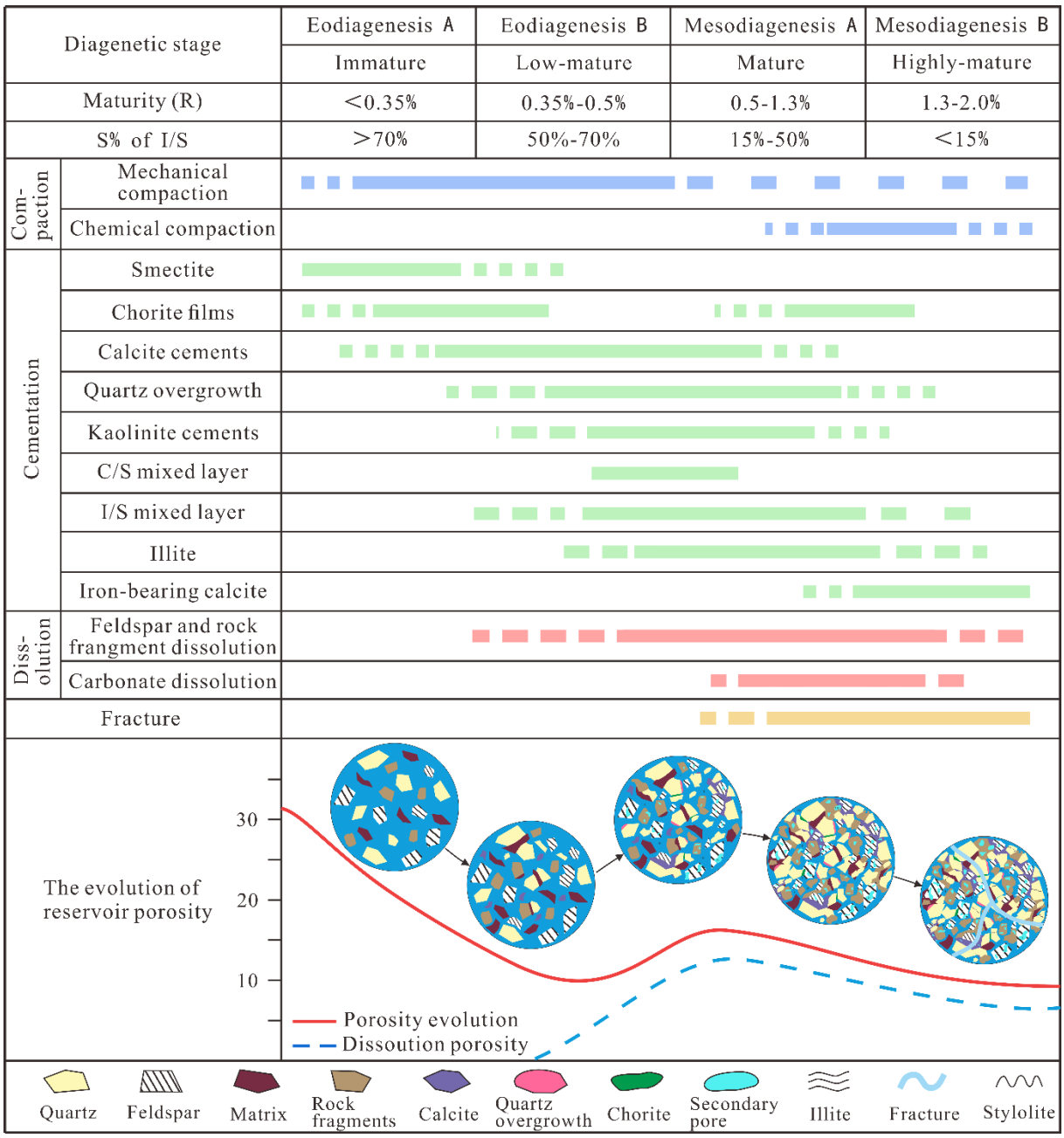

Figure 10. Diagenetic sequence of the Lower Jurassic reservoir in the Niudong area, northern margin of Qaidam Basin.

5.2. Diagenetic Stages and Paragenetic Sequence

Diagenetic stages can be divided according to rock structure, pore type, composition and distribution of authigenic minerals, the ratio of the smectite layer in the illite/smectite mixed layer, and vitrinite reflectance (Ro), among others [8,9]. The diagenesis characteristics of the Lower Jurassic strata in the Niudong area were as follows: (a) The contact types between debris particles included point contact, point-line contact, and some suture contact; (b) the enlargement degree of the quartz overgrowth was grades II–III, and calcite and kaolin cements were common; (c) secondary dissolved pores were the main pore types, followed by fractures; (d) the authigenic clay minerals mainly comprised kaolinite, followed by illite, illite/smectite mixed layer, and a small amount of chlorite, where kaolinite was mostly in the form of pages and worms, illite mostly in the form of flake, and the illite/smectite mixed layer was mostly honeycomb-like; (e) the ratio of smectite layer in

the illite/smectite mixed layer ranged from 5.0% to 35.0%, with an average of 7.8%; (f) the vitrinite reflectance (Ro) of organic matter in mudstone ranged from 0.876 to 1.379, with an average of 1.143; (g) feldspar and rock fragments were both dissolved; feldspar dissolution was more common, and was the main source of secondary pores; and (h) dark organic matter was visible in the pores, indicating that organic matter had entered the mature stage. Above all, according to the SY/T5477-2003 standard [58], the diagenetic stage of the Lower Jurassic strata in the Niudong area was in the middle diagenetic stage A–B (Figure 10).

The evolution of diagenesis is complicated. Through the thin section analysis and scanning electron microscopy, the authigenic mineral assemblage formed in different diagenetic stages and its distribution can be analyzed, and the diagenetic sequence can be accurately determined [59].

The main results of diagenetic sequence analysis in the study area were as follows: (a) Thin section analysis showed that the surface of the debris particles was surrounded by chlorite film, indicating that compaction occurred before chlorite formation (Figure 11a); (b) calcite filled the intergranular pores and the surrounding quartz particles were surrounded by chlorite film, indicating that calcite cementation occurred after the formation of chlorite film (Figure 11a); (c) quartz overgrowth and authigenic quartz particles often developed around quartz without the chlorite film, indicating that quartz overgrowth occurred after the formation of the chlorite film (Figure 11b,c); (d) kaolinite adhered on the surface of the quartz overgrowth, indicating that kaolinite was formed after quartz overgrowth (Figure 11b,c); (e) authigenic minerals such as booklet-like kaolinite and filamentous illite were visible in feldspar dissolution pores, indicating that the formation of authigenic minerals such as kaolinite and illite formed after feldspar dissolution (Figure 11d,e); (f) a small amount of iron-bearing calcite was visible in some feldspar dissolution pores and rock fragment dissolution pores, indicating that the cementation of iron-bearing calcite was after the dissolution of feldspar and rock fragments (Figure 11f,g); (g) dark organic matter could be seen in the feldspar or rock fragment dissolution pores, indicating that oil and gas filling and feldspar dissolution occurred simultaneously or occurred after dissolution (Figure 11h,i).

Based on the above analysis, the diagenetic sequence of the Lower Jurassic tight sandstone reservoir in the Niudong area of the northern margin of Qaidam Basin was preliminarily determined to be as follows: (a) early compaction, (b) early smectite formation, (c) early chlorite film formation, (d) early calcite cementation, (e) quartz overgrowth, (f) authigenic kaolinite formation, (g) illite/smectite mixed layer and chlorite/smectite mixed layer formation, (h) illite, (i) dissolution of feldspar and rock fragments (organic acid injection), (j) carbonate dissolution, (k) hydrocarbon filling, (l) iron-bearing calcite deposition, and (m) fracture occurrence (Figure 11). In addition, each stage in the process of reservoir diagenesis occurred alternately and repeatedly.

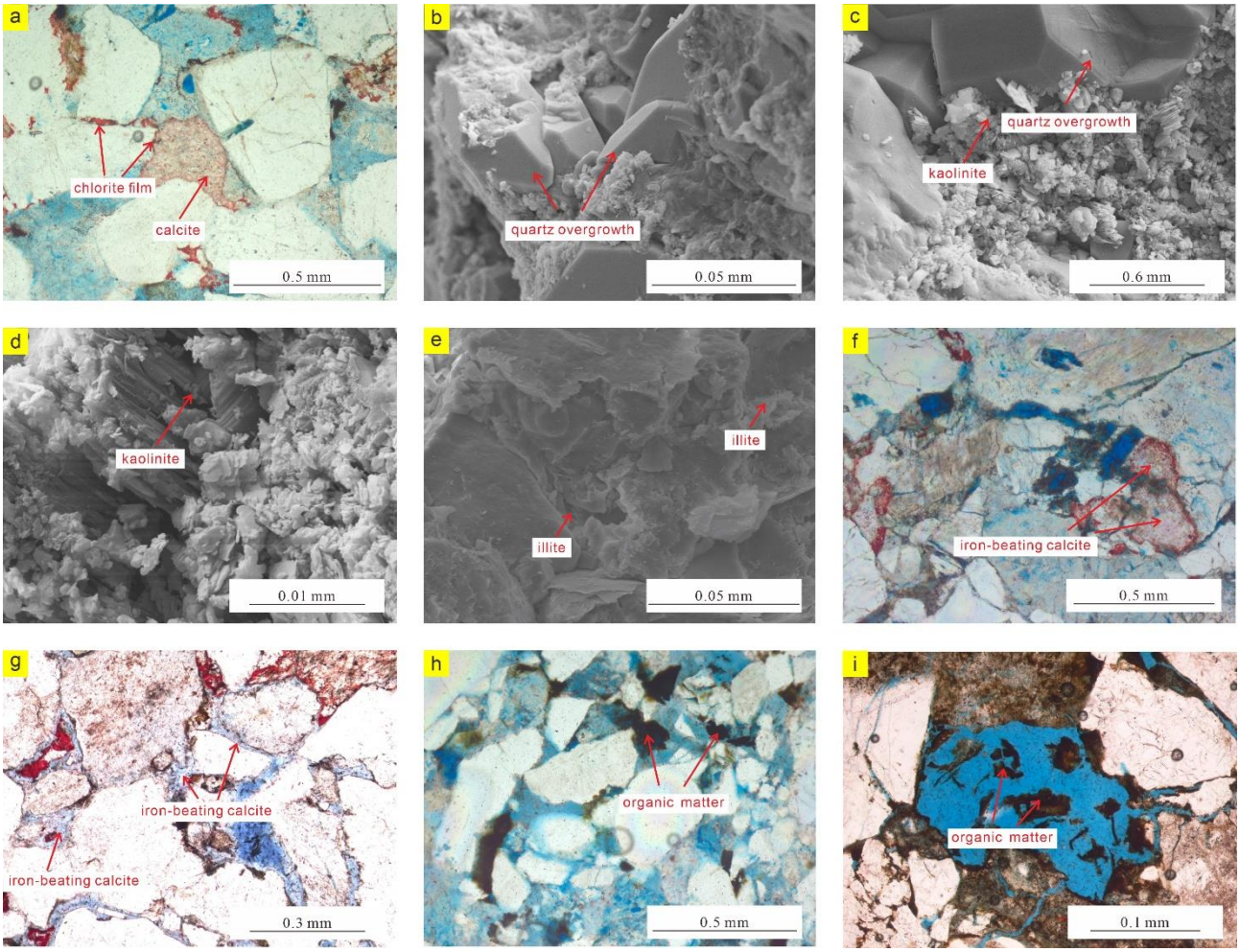

Figure 11. Characteristics of the paragenetic sequence of the Lower Jurassic reservoir in the Niudong area, northern margin of Qaidam Basin: (**a**) N1, 2227.9 m, chlorite film surrounded particles, calcite filled the intergranular pores; (**b**) N1, 2232.1 m, quartz overgrowth and authigenic quartz particles developed around quartz without chlorite film; (**c**) N1, 2231.7 m, quartz overgrowth and authigenic quartz particles developed around quartz without chlorite film, kaolinite adhered on the surface of the quartz overgrowth; (**d**) N102, 2115.8 m, kaolinite was visible in feldspar dissolution pores; (**e**) N102, 2038.6 m, illite were visible in feldspar dissolution pores; (**f**) N1, 2228.7 m, a small amount of iron-bearing calcite was visible in some feldspar dissolution pores and rock fragment dissolution pores; (**g**) EI2, 4050.5 m, iron-bearing calcite was visible in some feldspar dissolution pores and rock fragment dissolution pores; (**h**) N1, 2231.6 m, organic matter can be seen in feldspar or rock fragment dissolution pores; (**i**) N102, 2125.7 m, organic matter can be seen in rock fragment dissolution pores.

5.3. Controlling Factors of Reservoir Quality

The quality of low permeability sandstone reservoir is controlled by many factors, and the quality of the reservoir determines whether the reservoir can become an industrial oil and gas reservoir. Therefore, it is necessary to analyze and discuss the controlling factors of the Lower Jurassic reservoirs in the Niudong area to lay a foundation for later oil and gas exploration.

5.3.1. Control of Sedimentation

Sedimentary facies control the lithology, grain size, separation coefficient, primary porosity, and permeability of sand bodies, and then affect a series of subsequent diagenesis [60,61]. Generally, coarse-grained sandstone exhibits higher porosity and finer-grained sandstone has lower porosity. The cross plot shows that the correlation of porosity and permeability with the sorting coefficient (R^2 = 0.0044, R^2 = 0.0129) was lower than that

with average particle size (R^2 = 0.0294, R^2 = 0.0416) (Figure 12). However, no correlation was evident among these variables. The grain size and difference in sorting almost did not affect the physical properties of the reservoir, indicating strong heterogeneity of the study area, and strong effect of subsequent diagenesis on reservoir quality.

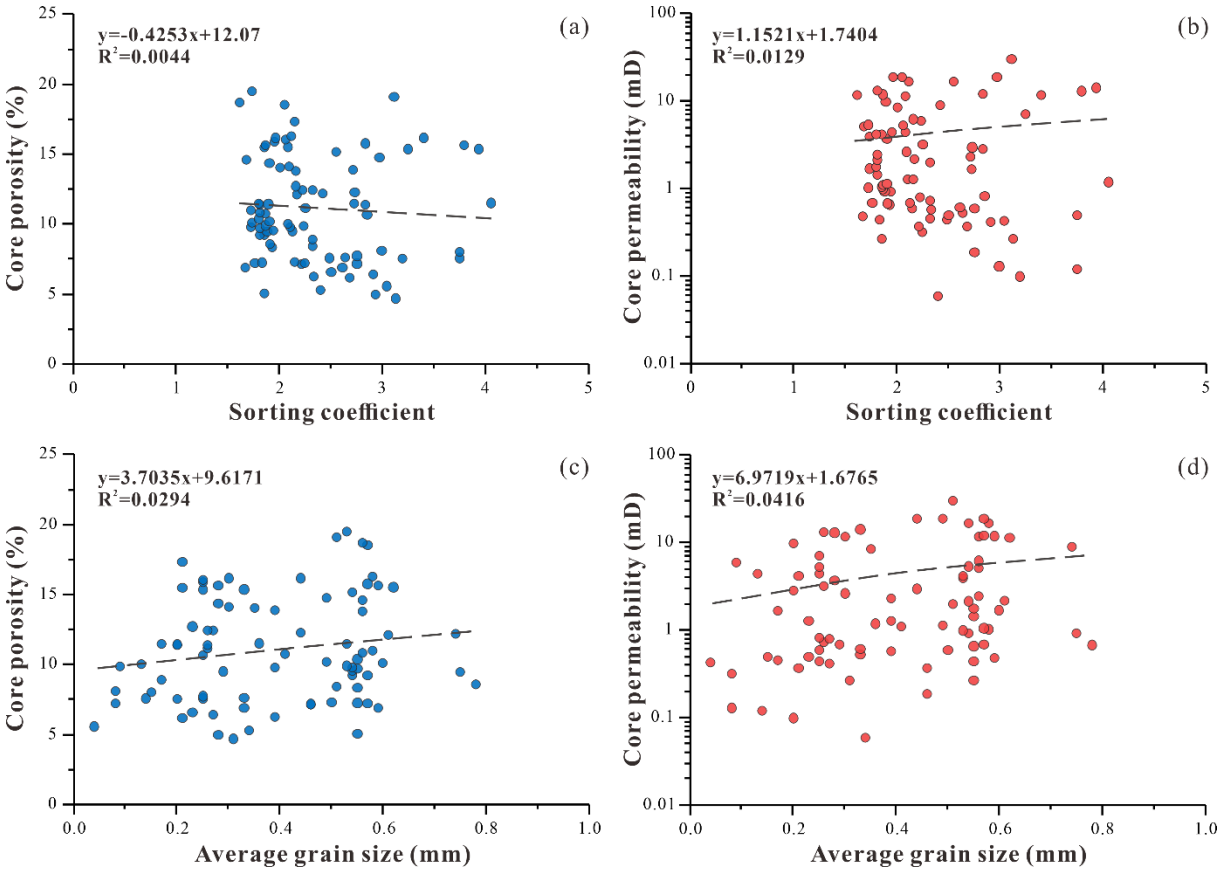

Figure 12. Relationship between sorting coefficient and average grain size and reservoir physical properties: (**a**) sorting coefficient and porosity; (**b**) sorting coefficient and permeability; (**c**) average grain size and porosity; (**d**) average grain size and permeability.

5.3.2. Control of Diagenesis

Compaction had the greatest influence on reservoir quality in the study area, followed by carbonate cementation, clay mineral cementation, and dissolution.

Compaction

According to the thin section analysis, most of the particles exhibited point contact or line contact, and the extrusion deformation of plastic particles (mica, etc.) occurred simultaneously, indicating that the study area has experienced strong compaction. According to the algorithm of the quantitative model of porosity evolution proposed by geologists Beard and Weyl in the 1970s [25], the initial porosity (Φ_1) of unconsolidated sandstone in the study area was 28.6–33.0% (average of 31.2%), which was much lower than the conventional 40.0%. At the same time, the relationship between intergranular pore volume (IGV) and cement content proposed by Ehrenberg (1989) (Figure 13) showed that during burial, the porosity loss rate caused by compaction ranged from 34.6–93.9% (average of 69.0%), and the porosity loss rate caused by cementation ranged from 6.2–64.7% (average of 25.7%). Dissolution increased porosity by 0.01–18.7% (average of 4.8%). These data show that compaction is the main factor influencing the reduction of physical properties in the

study area, and that cementation and dissolution are the main factors causing reservoir pore structure and reservoir heterogeneity.

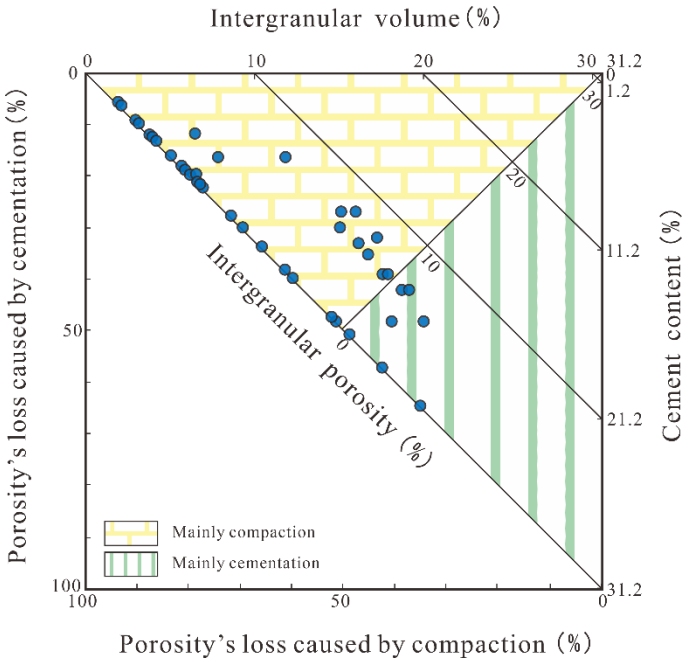

Figure 13. Influence of compaction and cementation on porosity evolution in the Niudong area, northern margin of Qaidam.

Calcite Cement

Carbonate cement is one of the common authigenic minerals in tight sandstone reservoirs, with a double impact on physical properties of the reservoir. On one hand, carbonate minerals occur as cement filling the intergranular pores, which reduce reservoir physical properties. On the other hand, carbonate cements formed in the early diagenetic stage improve the anti-compaction ability of sandstone and protect primary pores to a certain extent. In addition, in the process of dissolution, carbonate cement is easily dissolved and forms the secondary pores, thus improving the physical properties of the reservoir.

Calcite is the main carbonate cement in the low permeability sandstone reservoir of Lower Jurassic in the Niudong area. The scatter plot of calcite and porosity permeability indicates a complex correlation between the content of calcite and reservoir physical properties. When the content of calcite is below 4.0%, no obvious relationship is evident between the calcite content and porosity and permeability. However, when the content of calcite exceeds 4.0%, the content of calcite is negatively correlated with porosity and permeability (Figure 14). This is because when the calcite content is high, it can fill part of the pore space and reduce the physical properties of the reservoir. Based on thin section analysis, calcite evidently filled the intergranular pores in a continuous crystal manner, resulting in the complete loss of certain pores. At the same time, the authigenic calcite in the primary intergranular and dissolution pores not only reduces the reservoir space, but also reduces the reservoir permeability to a certain extent. Therefore, high calcite content destroys the physical properties of reservoirs.

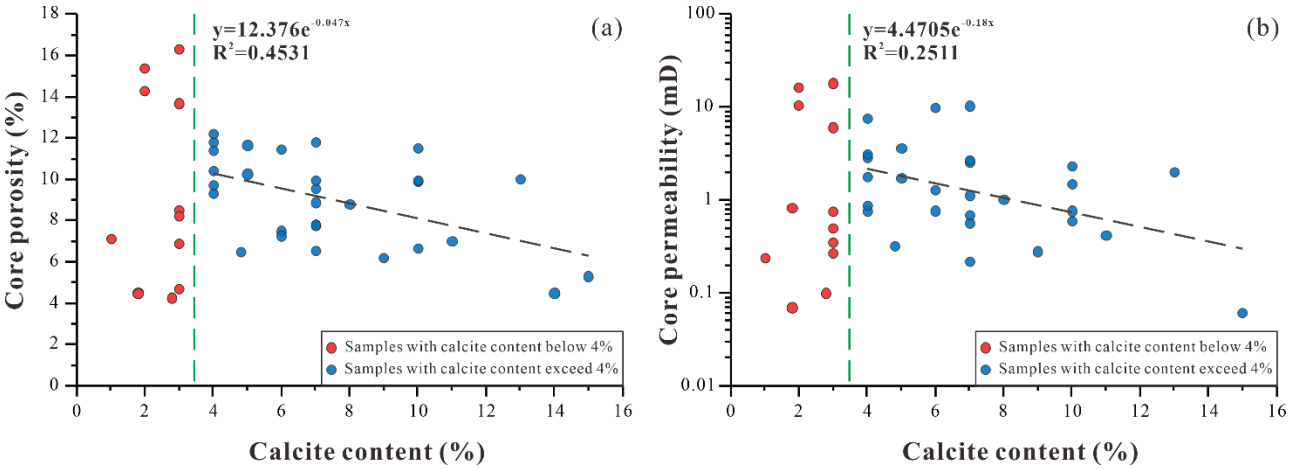

Figure 14. Relationship between calcite and the reservoir physical properties of the Lower Jurassic reservoir in the Niudong area, northern margin of Qaidam Basin: (**a**) calcite content and porosity; (**b**) calcite content and permeability.

Sources of carbonate cements can be measured by carbon ($\delta^{13}C$) and oxygen ($\delta^{18}O$) stable isotopes in carbonate cements [62–64]. The $\delta^{13}C$ value of inorganic carbon sources in nature ranges from −4.0‰ to 4.0 ‰, whereas the carbon in organic carbon is reduced carbon, which loses $\delta^{13}C$. Therefore, carbonate cements related to organic carbon often have low $\delta^{13}C$ values, which generally range from −35.0‰ to −4.0‰ [63,65]. In order to increase the reliability, the carbon and oxygen isotope measurement results of 12 samples (Table 2) and some data from Fu (2014) were analyzed together in this paper [66]. The results showed that the $\delta^{13}C$ values (V-PDB) in the study area ranged from −13.8‰ to −3.1‰, with an average of −9.9‰; and the $\delta^{18}O$ value (V-PDB) ranged from −19.3‰ to −11.1‰, with an average of −14.8‰. The relatively low negative $\delta^{13}C$ and $\delta^{18}O$ values indicate that the carbonate cement is derived from the oxidation or thermal decarboxylation of the organic matter and is the product of hydrocarbon generation by organic matter (Figure 15) [63,64].

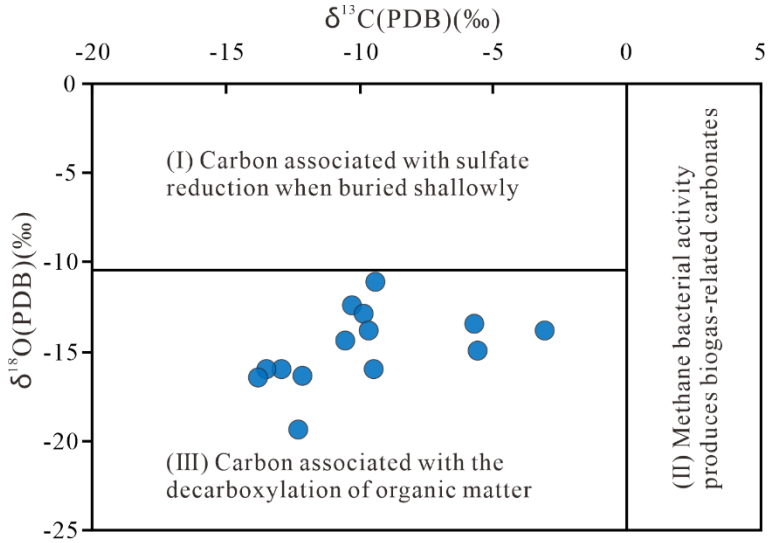

Figure 15. Carbon and oxygen isotopic composition of the calcite cements in the Niudong area (some data from [66]).

Clay Minerals

Clay minerals are also an important factor affecting reservoir quality [67], and it is also one of the important cementing materials in the study area. The effect of clay minerals on reservoir physical properties is generally attributed to the deposition of authigenic

clay minerals blocking the pore space of the reservoir or reducing the connectivity of the reservoir [16,24]. The cross plot of the total amount of clay minerals against porosity and permeability showed a certain negative correlation between them, and the correlation coefficients were 0.5282 and 0.4265 m respectively (Figure 16). This shows that clay minerals have a destructive effect on the physical properties of the reservoir, and greater influence on porosity than on permeability, which indicates that clay minerals in the study area generally affect the reservoir quality by filling the intergranular and intragranular pores.

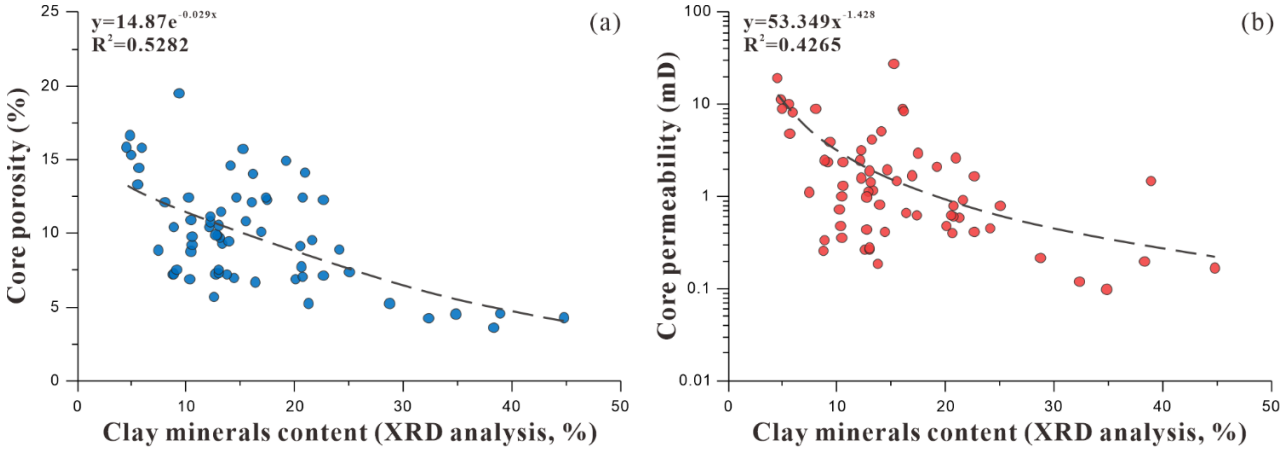

Figure 16. Total content of clay minerals with (**a**) core porosity and (**b**) core permeability of the Lower Jurassic reservoir in the Niudong area, northern margin of Qaidam Basin.

Different types of clay minerals have different effects on the physical properties of the reservoir. According to the X-ray diffraction results, the main clay mineral in the study area was kaolinite, followed by illite and the illite/smectite mixed layer, and the smectite, chlorite and chlorite/smectite mixed layer content were relatively low.

Feldspar content in this study area is high, and dissolved in the acidic environment to form authigenic kaolinite minerals. Authigenic kaolinite often fills primary intergranular pores or feldspar dissolved pores with page-like or worm-like aggregates [68,69]. In addition, the kaolinite aggregate has many intergranular pores; therefore, it can improve reservoir porosity to a certain extent. The content of kaolinite was positively correlated with porosity and permeability, and the correlation with porosity was more optimized than that with permeability. This is an indication that kaolinite contributes to reservoir quality by improving reservoir porosity (Figure 17a,b).

Scanning electron microscopy showed that illite mainly existed as honeycomb or in filamentous form, and formed bridging, filling between the particles; therefore, it could reduce the pore volume and narrow the throat. Generally, the higher the content of illite and the more developed the filamentous, the more inferior the reservoir quality. Illite mainly occurs in the form of honeycombs in the study area, and its correlations with porosity and permeability were not obvious. However, when the content of illite was high, it usually corresponded to lower porosity and permeability (Figure 17c,d).

Smectite and illite/smectite mixed layers were often in reticulate and honeycomb form, and were negatively correlated with porosity and permeability, but their correlation with porosity was more optimized than that with permeability (Figures 17e,f and 18b,c). The chlorite in the study area existed at the edge of the particles in the form of a thin film, which is beneficial to improving the anti-compaction performance of the particles, and can restrain quartz overgrowth as well as preserve certain primary pores. This has aa constructive effect on the physical properties of the reservoir (Figure 18a,b).

The chlorite/smectite mixed layer is not the main mineral in petroliferous basins in China, and is less common than the illite/smectite mixed layer [70]. It is only distributed in

a few formations in the Jianghan Basin, Tarim Basin, and Qaidam Basin, and its correlation with reservoir properties is not obvious (Figure 18e,f).

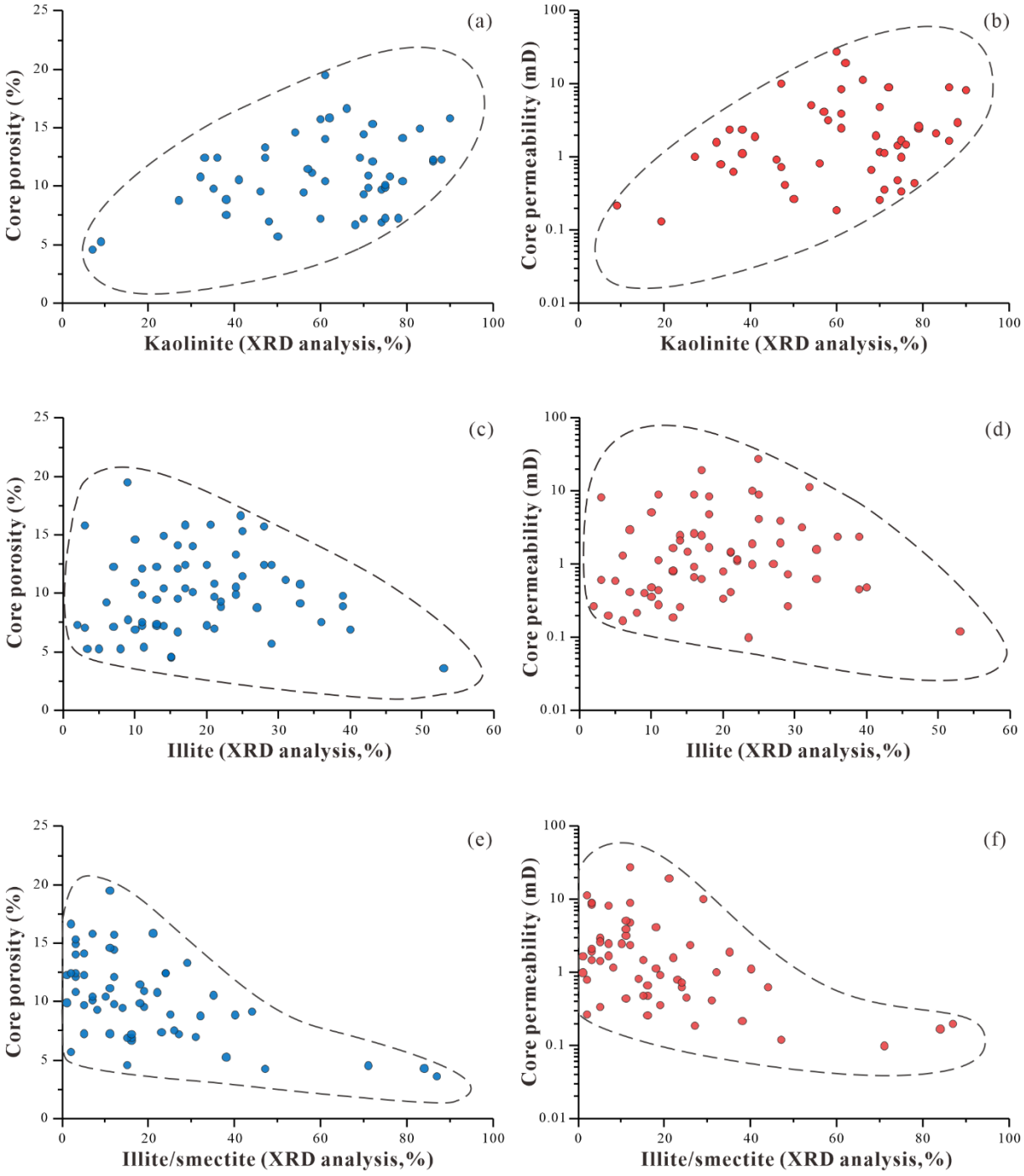

Figure 17. Relationship between different clay minerals and the reservoir physical properties: (**a**) kaolinite and porosity; (**b**) kaolinite and porosity; (**c**) illite and porosity; (**d**) illite and porosity; (**e**) illite/smectite mixed layers and porosity; (**f**) illite/smectite mixed layers and porosity.

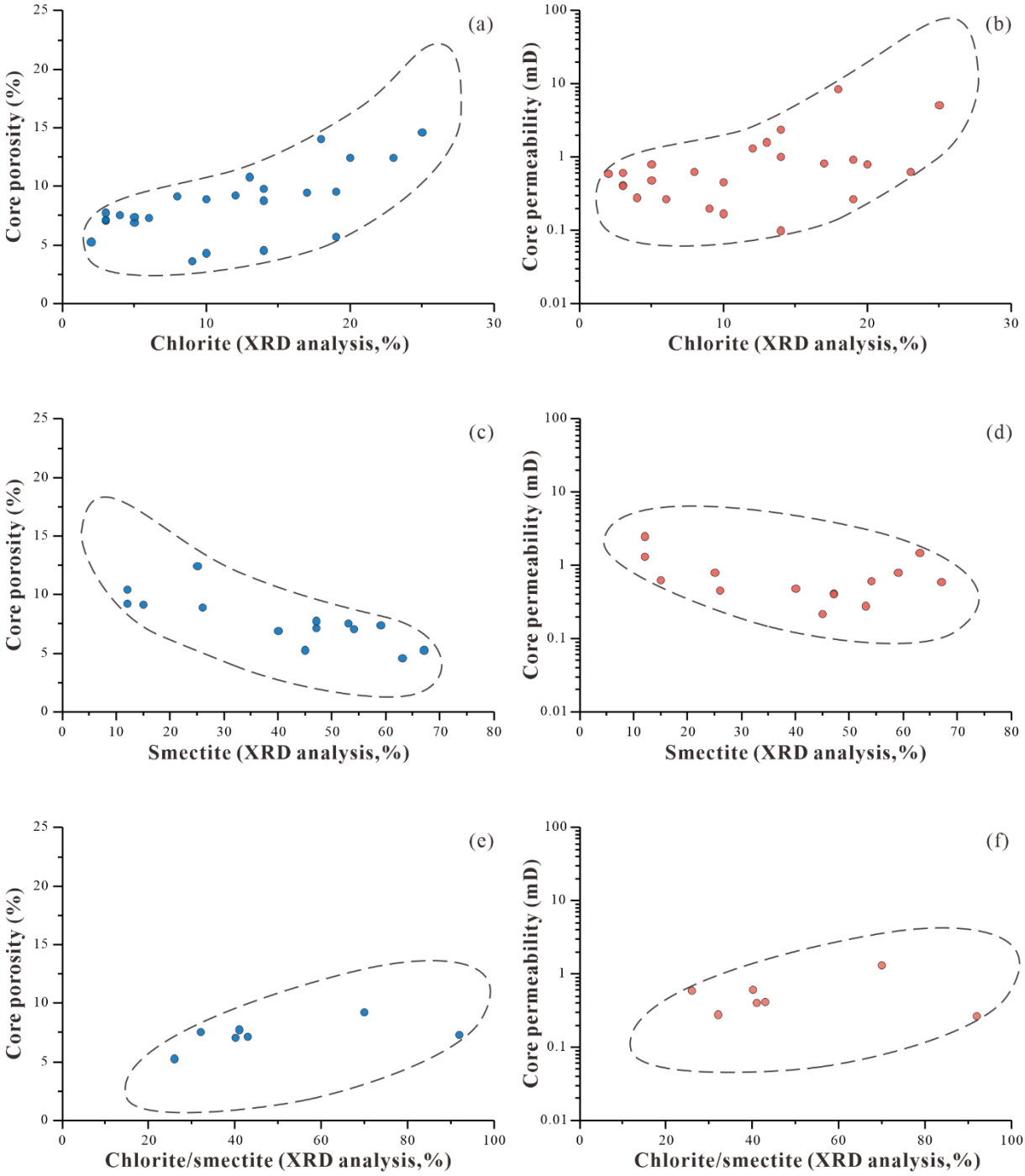

Figure 18. Relationship between different clay minerals and the reservoir physical properties: (**a**) Chlorite and porosity; (**b**) Chlorite and permeability; (**c**) Smectite and porosity; (**d**) Smectite and permeability; (**e**) Chlorite/smectite mixed layer and porosity; (**f**) Chlorite/smectite mixed layer and permeability.

Dissolution

Dissolution can form secondary pores and increase reservoir space as well as increase pore connectivity and reservoir permeability, which plays an important role in improving the physical properties of low permeability sandstone reservoirs [71]. Generally, dissolution is closely related to organic acids or deep hydrothermal fluids produced by source rocks, or atmospheric fresh water leaching near the surface after deposition or atmospheric fresh water leaching under unconformity during the uplift stage [33,72,73]. The burial history

map of the Niudong area (Figure 19) shows that the Lower Jurassic reservoir was not uplifted to the surface, and no atmospheric precipitation leaching occurred. Therefore, the dissolution of the study area should be caused by other factors.

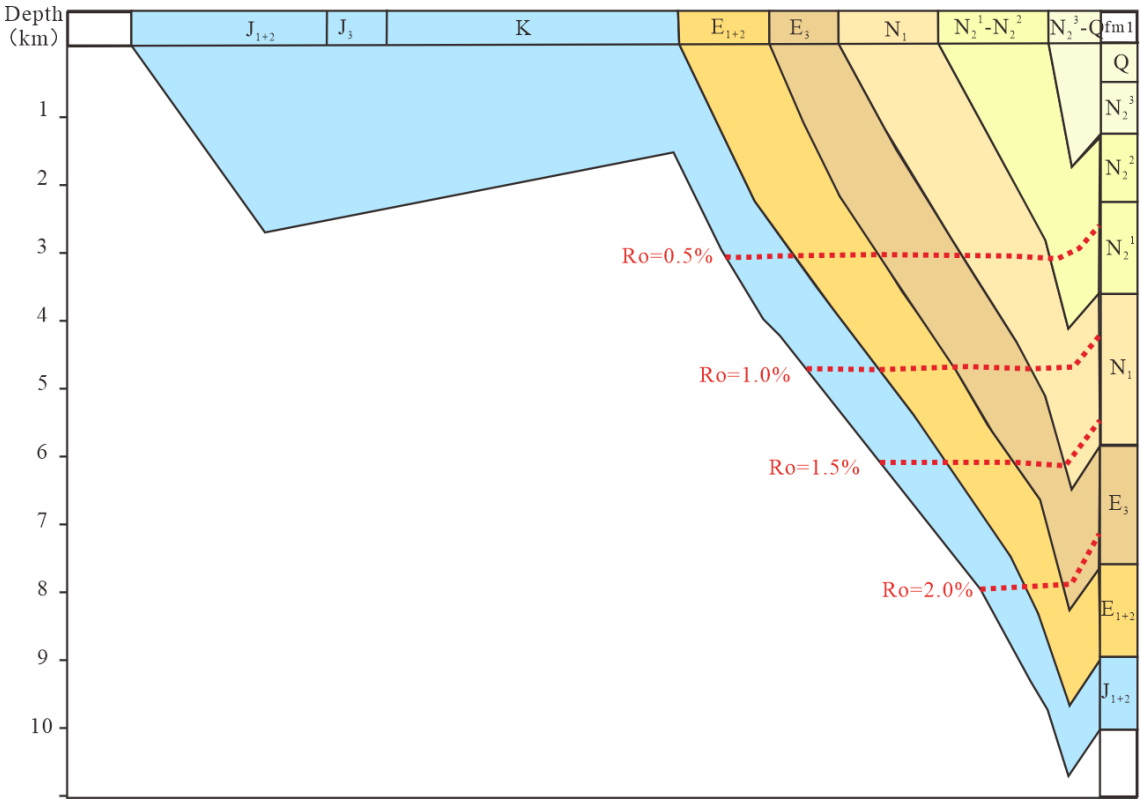

Figure 19. Burial history of the Lower Jurassic reservoir in the Niudong area, northern margin of Qaidam Basin, China (modified from [74]).

The Niudong area in the northern margin of Qaidam Basin has experienced strong dissolution due to its good conditions for dissolution, these favorable conditions are as follows:

(a) The sandstone reservoir in the study area is in the stage of middle diagenesis, and the source rocks are mature. In the process of conversion from organic matter to hydrocarbons, a large amount of CO_2 was released and organic acids such as carboxylic acids were formed [75], Moreover the Lower Jurassic reservoirs in the Niudong area included coal-bearing strata, and the organic acids produced by coal-bearing strata were generally several times higher than those of other source rocks [76], thus availing abundant organic acids for dissolution;

(b) Due to the long-term uplift caused by Yanshan movement, the strata between the Lower Jurassic strata and Paleogene strata in the Niudong area were eroded to form regional unconformity, and the unconformity was widely developed [36];

(c) Some acidic fluids can also be produced during the conversion of clay materials. For example, H^+ can be generated in the conversion process from smectite to illite, which increases the acidity of the diagenetic fluid and promotes the occurrence of dissolution to a certain extent [77];

(d) During the conversion process of clay action, smectite can discharge a certain amount of interlayer water into the pores and promote the migration of organic acids; and

(e) The mineral composition of sandstone shows that the sandstone in the study area contains a large number of unstable materials such as feldspar, volcanic debris, and carbonate detritus, which provides a certain material basis for dissolution. In acidic fluid,

soluble materials such as feldspar and carbonate minerals are dissolved easily and produce secondary pores [78].

Dissolution mainly occurs in feldspar in the study area, and the dissolution degree of feldspar is high. In addition, a few feldspar particles completely dissolved to form mold pores. Secondary dissolved pores were positively correlated with core porosity (Figure 20a), core permeability (Figure 20b), and total porosity of the thin section (Figure 20c) (R^2 = 0.4681, R^2 = 0.3071, R^2 = 0.7125). Dissolution can be inferred to play an important role in improving the physical properties of reservoirs.

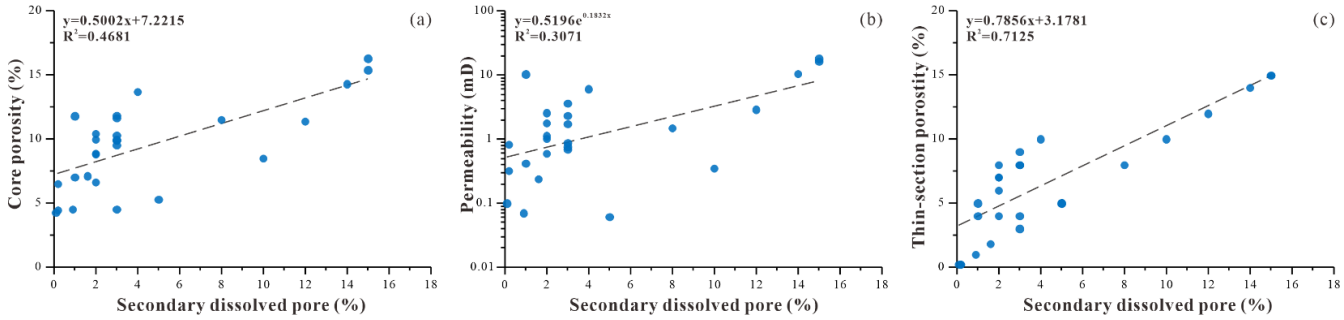

Figure 20. Cross-plots showing the relationship between secondary dissolved pore and (**a**) core porosity, (**b**) core permeability, and (**c**) thin-section porosity.

5.3.3. Fracture

Tectonically, the Niudong area is characterized by a large nose uplift structure that plunges from piedmont to basin, and is mainly controlled by the Eboliangdong and Eboliangxi faults. The Niudong nose bulge is roughly along the NWW trend and dips to the southeast, and Jurassic strata are widely distributed in the nose bulge. Based on the frequent tectonic movements, fractures are relatively developed in the Niudong area. The existence of fractures allows for the further dissolution of unstable minerals and the enlargement of primary intergranular pores, which form the main channel and storage space for natural gas migration, and are crucial to the improvement in the physical properties of low permeability sandstone reservoirs [79,80].

Generally, micro-fractures with openings that are greater than 0.1 μm can become effective fractures for oil and gas migration [81]. Observations from the thin section showed that the micro-fracture opening in the Niudong area ranged from 0.4 to 115.0 μm. Therefore, it can be used as an effective oil and gas reservoir space and migration channel.

Thin section analysis showed that the permeability of the sample with fractures was higher than that of the sample without fractures (Figure 21a). Moreover, the fractures exhibited a strong positive correlation with the core permeability, core porosity, and porosity of the thin section, and its correlation with permeability was more optimized than that with porosity (Figure 21b–d). The above results show that the development of fractures can improve the reservoir space, and greatly improve the connectivity of pores, which play an important role in improving the physical properties of reservoirs in the study area.

The feldspar content was positively related to the fracture content, and the debris content had no obvious relationship with fractures (Figure 21e,f). This shows that plastic materials such as debris are prone to extrusion deformation under stress, whereas rigid particles such as feldspar break easily, forming a cleavage crack. At the same time, the cleavage crack further expands to form effective fractures under the corrosion of acidic substances, which improves the physical properties of reservoirs.

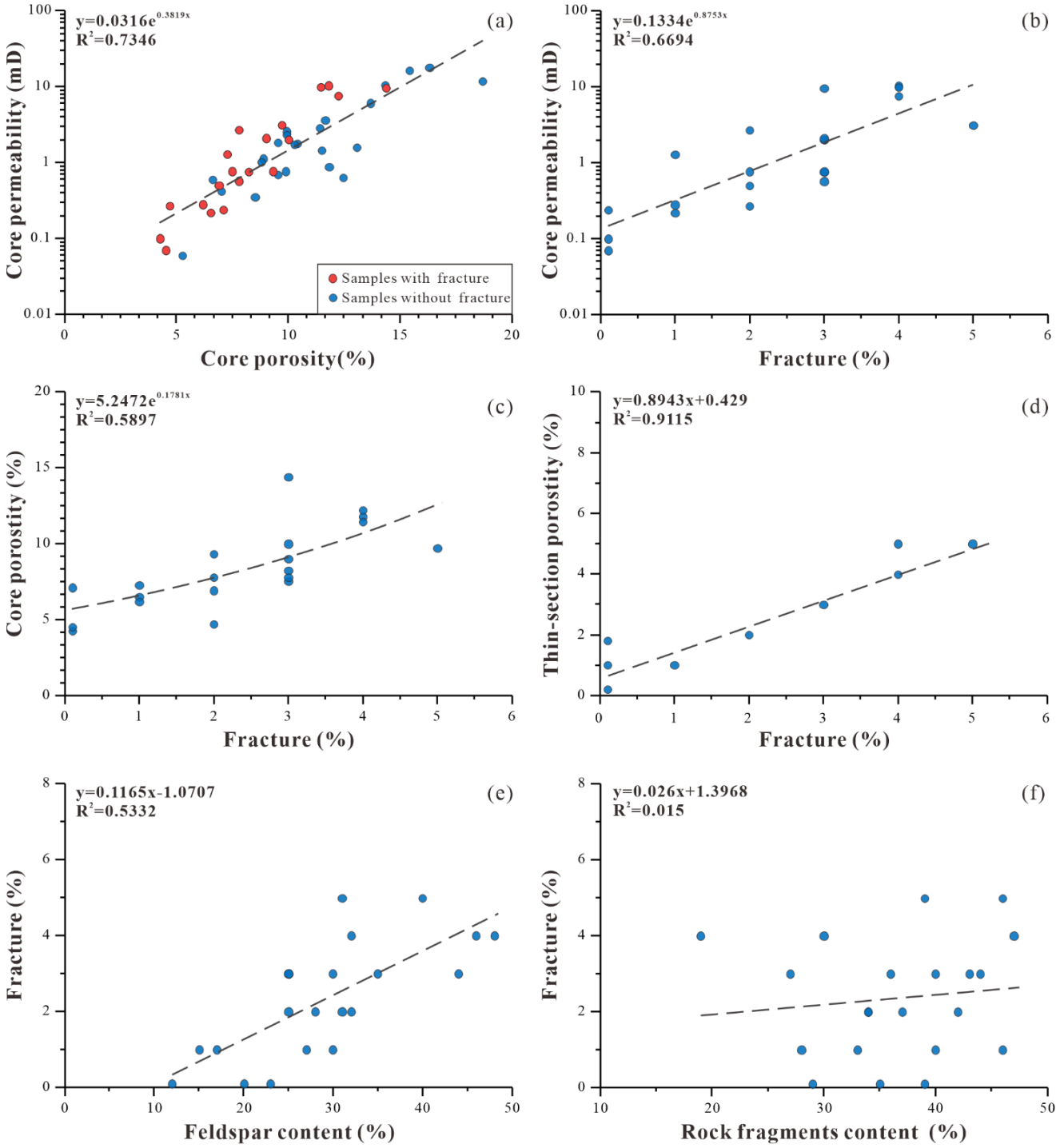

Figure 21. Relationship between the fractures and core permeability, core porosity, thin-section porosity, feldspar content, and rock fragment content. (**a**) core porosity and core permeability; (**b**) fracture and core permeability; (**c**) fracture and core porosity; (**d**) fracture and thin-section porosity; (**e**) feldspar content and fracture; (**f**) rock fragments content and fracture.

6. Conclusions

(1) Feldspathic litharenite and lithic arkose are the main types of sandstone type in the Niudong area of the northern margin of Qaidam Basin, followed by arkose and litharenite. The sorting is ordered from medium to poor. In addition, the porosity was low (0.0–19.5%) with an average of 9.9%, the permeability was low (0.0–32.4 mD) with an average of 3.8 mD, and heterogeneity of the reservoir was strong. The main reservoir space comprised secondary pores, followed by fractures, and a small amount of residual grains was observed. Secondary pores included intergranular and intragranular dissolved pores.

(2) The reservoir quality in the study area is not greatly affected by sedimentation, and is mainly controlled by diagenesis. The Lower Jurassic reservoirs in the Niudong area have undergone complex diagenesis, and the diagenesis types mainly include compaction, cementation, and dissolution. At present, the reservoir is in the middle diagenetic stage (A–B), and the diagenetic sequence is as follows: (a) early compaction, (b) early smectite formation, (c) early chlorite film formation, (d) early calcite cementation, (e) quartz secondary enlargement, (f) authigenic kaolinite formation, (g) illite–smectite mixed layer and chlorite–smectite mixed layer formation, (h) illite, (i) dissolution in feldspar or rock fragments (organic acid injection), (j) carbonate dissolution, (k) hydrocarbon filling, (l) iron-bearing calcite deposition, and (m) fracture occurrence.

(3) The quantitative analysis of pore evolution showed that the porosity loss rate caused by compaction was 69.0% on average, and the porosity loss rate caused by cementation was 26.7% on average. Porosity increased by dissolution was 4.8% on average. Compaction is the main factor influencing the decrease in reservoir physical properties in the study area, and cementation and dissolution are the main causes of reservoir pore structure and reservoir heterogeneity.

(4) The influence of cementation on the reservoir is complex, and the types of cements mainly include carbonate cement and authigenic clay. Calcite is the main carbonate cement in the study area. When the content of calcite is below 4.0%, its content has no obvious relationship with the physical properties. When the content of calcite exceeds 4.0%, the intergranular pores and secondary solution pores will be filled and the physical properties of the reservoir reduced. The source of carbonate cement in the study area is related to the thermal deacidification of organic matter. Different types of clay minerals have different effects on the reservoir; the illite/smectite mixed layer and illite reduced the porosity of the reservoir by filling primary intergranular pores and secondary solution pores. Chlorite film can improve the compaction resistance of particles and restrain quartz overgrowth to improve the physical properties.

(5) The Niudong area has strong dissolution and remarkable conditions for dissolution, and the dissolution mainly occurred in feldspar. Dissolution can form secondary pores and increase reservoir space as well as increase reservoir permeability, which plays an important role in improving the physical properties of low permeability sandstone reservoirs. In addition, the Niudong area is characterized by a large nose uplift structure, and fractures are relatively developed. The micro-fracture openings in the Niudong area ranged from 0.4 to 115.0 μm, so fractures can be used as an effective oil and gas reservoir space and migration channel. Furthermore, the existence of fractures provides favorable conditions for the uninterrupted entry of acidic fluid into the reservoir promotes the occurrence of dissolution. Above all, dissolution and fractures play an important role in improving reservoir physical properties in low permeability sandstone reservoirs of the Lower Jurassic in the Niudong area.

Author Contributions: Conceptualization, W.L. and T.F. methodology, W.L., Z.G., Z.W. and Y.L.; formal analysis, W.L.; investigation, W.L., X.Z., H.Z. and F.C.; resources, Z.W.; data curation, Y.L., X.Z., H.Z. and F.C.; writing—original draft preparation, W.L.; writing—review and editing, T.F. and Z.G.; supervision, T.F.; funding acquisition, T.F. All authors have read and agreed to the published version of the manuscript.

Funding: This work was supported by the National Natural Science Foundation of China (grant 41972130); the PetroChina Innovation Foundation (grant 2019D-5007-0103); the Strategic Priority Research Program of the Chinese Academy of Sciences (grant XDA14010201-02); the Sinopec Science and Technology Project (Grant GSYKY-B09-33); and a grant from the Exploration and Development Research Institute of the Qinghai Oilfield (grant 2018-Technique-Exploration-02).

Data Availability Statement: Not applicable. The data are not publicly available due to the privacy issues.

Acknowledgments: We also thank the Exploration and Development Research Institute of the Qinghai Oilfield Company for supporting this study. We thank Elsevier (https://webshop.elsevier.com/, accessed on 10 February 2021) for its linguistic assistance during the preparation of this manuscript.

Conflicts of Interest: The authors declare that they have no known competing financial interests or personal relationships that could have appeared to influence the work reported in this paper.

References

1. Adibhatla, B.; Mohanty, K.K. Parametric analysis of surfactant-aided imbibition in fractured carbonates. *J. Colloid Interface Sci.* **2008**, *317*, 513–522. [CrossRef]
2. Li, S.; Zhang, K.; Jia, N.; Liu, L. Evaluation of four CO2 injection schemes for unlocking oils from low-permeability formations under immiscible conditions. *Fuel* **2018**, *234*, 814–823. [CrossRef]
3. Wang, L.; Tian, Y.; Yu, X.; Wang, C.; Yao, B.; Wang, S.; Winterfeld, P.H.; Wang, X.; Yang, Z.; Wang, Y.; et al. Advances in improved/enhanced oil recovery technologies for tight and shale reservoirs. *Fuel* **2017**, *210*, 425–445. [CrossRef]
4. Shanley, K.W.; Cluff, R.M.; Robinson, J.W. Factors controlling prolific gas production from low-permeability sandstone reservoirs: Implications for resource assessment, prospect development, and risk analysis. *AAPG Bull.* **2004**, *88*, 1083–1121. [CrossRef]
5. Zhiqiang, Z.; Junwei, Z. Advances in exploration and exploitation technologies of low-permeability oil and gas. *Adv. Earth Sci.* **2009**, *24*, 854–864.
6. Hu, W.; Wei, Y.; Bao, J. Development of the theory and technology for low permeability reservoirs in China. *Pet. Explor. Dev.* **2018**, *45*, 685–697. [CrossRef]
7. Li, Q.; Zhang, L.; Husein, M. Production performance by polymer conformance control in ultra-low permeability heterogeneous sandstone reservoirs produced under their natural energy. *J. Pet. Sci. Eng.* **2020**, *193*, 107348. [CrossRef]
8. Li, P. *Microscopic Pore Structure Characterization and Production Characteristic Analysis of Low-Permeability Sandstone Reservoir: A Case Study and Chang. 4+5 and Chang. 6 Reservoir of T Area in Jiyuan Oilfield*; Northwest University: Xi'an, China, 2019.
9. Xinzhi, Z. *Characteristics and Grading Evaluation of Low Permeability Reservoir in the Longdong Region, Ordos Basin*; China University of Geoscience: Wuhan, China, 2012.
10. Hu, W. The present and future of low permeability oil and gas in China. *Eng. Sci.* **2009**, *11*, 29–37.
11. Zou, C.; Zhu, R.K.; Wu, S.T.; Yang, Z.; Tao, S.Z.; Yuan, X.; Hou, L.; Yang, H.; Xu, C.; Li, D.; et al. Types, characteristics, genesis and prospects of conventional and unconventional hydrocarbon accumulations: Taking tight oil and tight gas in China as an instance. *Acta Pet. Sin.* **2012**, *33*, 173–187.
12. Zou, C.; Yang, Z.; Zhang, G.; Hou, H.; Zhu, R.K.; Tao, S.Z.; Yuan, X.J.; Dong, D.Z.; Wang, Y.M.; Guo, Q.L.; et al. Conventional and unconventional petroleum "orderly accumulation": Concept and practical significance. *Pet. Explor. Dev.* **2014**, *41*, 14–30. [CrossRef]
13. Zhao, J.Z.; Wu, S.B.; Wu, F.L. The classification and evaluation criterion of low permeability reservoir: An example from Ordos Basin. *Lithol. Reserv.* **2007**, *3*, 28–31.
14. Li, D. *The Development of Low-Permeability Sandstone Oilfields*; Petroleum Industry Press: Beijing, China, 1997; p. 354. (In Chinese)
15. Jiang, L.Z.; Gu, J.Y.; Guo, B. Characteristics and mechanism of low permeability clastic reservoir in Chinese Petroliferous Basin. *Acta Sedimentol. Sin.* **2004**, *22*, 13–18.
16. Wang, G.; Chang, X.; Yin, W.; Li, Y.; Song, T. Impact of diagenesis on reservoir quality and heterogeneity of the Upper Triassic Chang 8 tight oil sandstones in the Zhenjing area, Ordos Basin, China. *Mar. Pet. Geol.* **2017**, *83*, 84–96. [CrossRef]
17. Katz, B.; Lin, F. Lacustrine basin unconventional resource plays: Key differences. *Mar. Pet. Geol.* **2014**, *56*, 255–265. [CrossRef]
18. Taylor, T.R. Sandstone diagenesis and reservoir quality prediction: Models, myths, and reality. *Am. Assoc. Pet. Geol. Bull.* **2010**, *94*, 1093–1132. [CrossRef]
19. Hu, Z.W.; Huang, S.J.; Li, X.N.; Qi, S.C.; Lang, X.G. Influence of pore-throat sizes on reservoir quality of low-permeability sandstone of Chang 2 oil-bearing bed from the Jiyuan, Ordos Basin. *Xinjiang Geol.* **2012**, *30*, 438–441.
20. Zeng, D.Q.; Li, S.Z. Types and characteristics of low permeability sandstone reservoirs in China. *Acta Pet. Sin.* **1994**, *1*, 38–46.
21. Spencer, C.W. Review of characteristics of low-permeability gas-reservoirs in western united states. *Am. Assoc. Pet. Geol. Bull.* **1989**, *73*, 613–629.

22. Zhou, Y.; Ji, Y.; Xu, L.; Che, S.; Niu, X.; Wan, L.; Zhou, Y.; Li, Z.; You, Y. Controls on reservoir heterogeneity of tight sand oil reservoirs in Upper Triassic Yanchang Formation in Longdong Area, southwest Ordos Basin, China: Implications for reservoir quality prediction and oil accumulation. *Mar. Pet. Geol.* **2016**, *78*, 110–135. [CrossRef]
23. Lai, J.; Wang, G.; Ran, Y.; Zhou, Z.; Cui, Y. Impact of diagenesis on the reservoir quality of tight oil sandstones: The case of Upper Triassic Yanchang Formation Chang 7 oil layers in Ordos Basin, China. *J. Pet. Sci. Eng.* **2016**, *145*, 54–65. [CrossRef]
24. Bjorlykke, K. Relationships between depositional environments, burial history and rock properties. Some principal aspects of diagenetic process in sedimentary basins. *Sediment. Geol.* **2014**, *301*, 1–14. [CrossRef]
25. Beard, D.C.; Weyl, P.K. Influence of texture on porosity and permeability of unconsolidated sand. *Am. Assoc. Pet. Geol. Bull.* **1973**, *57*, 349–369.
26. Ajdukiewicz, J.M.; Lander, R.H. Sandstone reservoir quality prediction: The state of the art. *Am. Assoc. Pet. Geol. Bull.* **2010**, *94*, 1083–1091. [CrossRef]
27. Ma, Y.; Li, W.; Ouyang, Z.; Zhang, D.; Meng, H. Reservoir characteristics and main control factors of Chang 6 oil-bearing formation in Western Nanliang Area of Ordos Basin. *Geol. Bull. China* **2013**, *32*, 1471–1476.
28. Lai, J.; Wang, G.W.; Xin, Y.; Zhou, L.; Xiao, C.; Han, C.; Zheng, X.; Wu, Q. Diagenetic facies analysis of tight sandstone gas reservoir of Bashijiqike Formation in Kuqa Depression. *Nat. Gas. Geosci.* **2014**, *25*, 1019–1032.
29. Shi, Y.J.; Xiao, L.; Mao, Z.Q.; Guo, H.P. An identification method for diagenetic facies with well logs and its geological significance in low-permeability sandstones: A case study on Chang 8 reservoirs in the Jiyuan region, Ordos Basin. *Acta Pet. Sin.* **2011**, *32*, 820–828.
30. Dos Anjos, S.M.C.; de Ros, L.F.; de Souza, R.S.; de Assis, S.C.M.; Sombra, C.L. Depositional and diagenetic controls on the reservoir quality of Lower Cretaceous Pendencia sandstones, Potiguar rift basin, Brazil. *Am. Assoc. Pet. Geol. Bull.* **2000**, *84*, 1719–1742.
31. Gier, S.; Worden, R.H.; Johns, W.D.; Kurzweil, H. Diagenesis and reservoir quality of Miocene sandstones in the Vienna Basin, Austria. *Mar. Petr. Geol.* **2008**, *25*, 681–695. [CrossRef]
32. Bjorlykke, K.; Ramm, M.; Saigal, G.C. Sandstone diagenesis and porosity modification during basin evolution. *Geol. Rundsch.* **1989**, *78*, 243–268. [CrossRef]
33. Schmidt, V.; McDonald, D.A. The role of secondary porosity in the course of sandstone diagenesis. *Am. Assoc. Pet. Geol. Bull.* **1979**, *26*, 8.
34. Fu, J.H.; Wei, X.S.; Nan, J.X.; Shi, X.H. Characteristics and origin of reservoirs of gas fields in the Upper Paleozoic tight sandstone, Ordos Basin. *J. Palaeogeogr.* **2013**, *15*, 529–538.
35. Shou, J.F.; Zhang, H.L.; Yang, S.; Wang, X.; Zhu, G.H.; Si, C.S. Diagenetic mechanisms of sandstone reservoirs in China and gas-bearing basins. *Acta Pet. Sin.* **2006**, *22*, 2165–2170.
36. Ren, C.; Gao, X.; Zhang, Y.; Wang, B.; Hou, Z.; He, F.; Zhang, T. Structural characteristics and hydrocarbon control action of Paleogene/Jurassic unconformity in Niudong area, North Margin of Qaidam Basin. *Acta Geosci. Sin.* **2019**, *40*, 795–804.
37. Xu, Z.; Tian, J.X.; Yang, G.R.; Bo, W.; Guo, Z.Q.; Wang, W.; Zhang, H.L. Structure characteristics and petroleum geological significance of Jurassic sags at the northern margin of Qaidam Basin. *China Pet. Explor.* **2017**, *22*, 54–63.
38. Wu, Y.Y.; Song, Y.; Jia, C. Sedimentary features in a sequence stratigraphic framework in the north area of Qaidam Basin. *Earth Sci. Front.* **2005**, *12*, 195–203.
39. Wu, Z.; Wang, B.; Zhao, J.; Zou, K.; Zhou, F.; Xiong, K. Diagenesis of Jurassic and its influence on reservoir properties in Niudong area, Eastern Altun Foreland. *Lithol. Reserv.* **2016**, *28*, 58–64.
40. Zhang, W.; Jian, X.; Fu, L.; Feng, F.; Guan, P. Reservoir characterization and hydrocarbon accumulation in late Cenozoic lacustrine mixed carbonate-siliciclastic fine-grained deposits of the northwestern Qaidam basin, NW China. *Mar. Pet. Geol.* **2018**, *98*, 675–686. [CrossRef]
41. Lv, B.; Zhang, Y.; Yang, S. Characteristics of structural system and its implication for formation dynamics in Qaidam Basin. *Geol. Rev.* **2011**, *57*, 167–174.
42. Zhu, L.; Wang, C.; Zheng, H.; Xiang, F.; Yi, H.; Liu, D. Tectonic and sedimentary evolution of basins in the northeast of Qinghai-Tibet Plateau and their implication for the northward growth of the plateau. *Palaeogeogr. Palaeoclim. Palaeoecol.* **2006**, *241*, 49–60. [CrossRef]
43. Wang, J.; Zhang, D.; Yang, S.; Li, X.; Shi, Y.; Cui, J.; Zhang, P.; Wang, Y.; Yi, D.; Chang, H. Sedimentary characteristics and genesis of the salt lake with the upper member of the Lower Ganchaigou Formation from Yingxi sag, Qaidam Basin. *Mar. Pet. Geol.* **2020**, *111*, 135–155. [CrossRef]
44. Song, J.; Liao, J. Structure characteristics and petroliferous regions in the Chaidamu (Tsdam) Basin. *Acta Pet. Sin.* **1982**, *8*, 14–23.
45. Hu, S.-Q.; Cao, Y.-J.; Huang, J.-X. Discussion on formation and evolution of Jurassic basin prototype of Qaidam basin. *Pet. Geol. Exp.* **1999**, *21*, 189–195.
46. Tian, J.; Li, J.; Pan, C.; Tan, Z.; Zeng, X.; Guo, Z.; Wang, B.; Zhou, F. Geochemical characteristics and factors controlling natural gas accumulation in the northern margin of the Qaidam Basin. *J. Pet. Sci. Eng.* **2018**, *160*, 219–228. [CrossRef]
47. Guo, Z.; Sun, P.; Li, J.; Zhang, L.; Liu, W.; Tian, J.; Zhang, S.; Zeng, S. Natural gas types, distribution controlling factors, and future exploration in the Western Qaidam Basin. *Acta Geol. Sin.* **2014**, *88*, 1214–1226. [CrossRef]
48. Dickson, J.A.D. Carbonate identification and genesis as revealed by staining. *J. Sediment. Pet.* **1966**, *36*, 491–505.

49. Hu, T.; Pang, X.; Yu, S.; Wang, X.; Pang, H.; Guo, J.; Jiang, F.; Shen, W.; Wang, Q.; Xu, J. Hydrocarbon generation and expulsion characteristics of Lower Permian P(1)f source rocks in the Fengcheng area, northwest margin, Junggar Basin, NW China: Implications for tight oil accumulation potential assessment. *Geol. J.* **2016**, *51*, 880–900. [CrossRef]
50. Folk, R.L. *Petrology of Sedimentary Rocks*; Hemphill Publishing Company: Austin, TX, USA, 1980; p. 182.
51. Yu, X. *Reservoir Sedimentology of Clastic Rocks*; Petroleum Industry Press: Beijing, China, 2000; p. 352.
52. Zhou, Y. Research on diagenesis in Chang 8 Reservoir of Zhiluo Oilfield in Ordos Basin. *Ground Water* **2013**, *35*, 208–211.
53. Fu, W. Influence of clay minerals on sandstone reservoir properties. *J. Palaeogeogr.* **2000**, *2*, 59–68.
54. Wang, X.Z.; Zhang, L.X.; Yu, B.; Zhou, L.D.; Yin, J.T. Diagenesis of Shan-2 Member of Shanxi Formation in Yanchang Oil-Gas Field in Ordos Basin. *Geol. Sci. Technol. Inf.* **2013**, *32*, 114–118.
55. Zhao, X. *Analysis of Clay Minerals Content and Clay Minerals*; China Ocean Press: Beijing, China, 1990; p. 341.
56. Li, Y. *Tight Sandstone Reservoir Microscopic Pore Throat Structure Fine characterization: With G3 and G4 of Gaotaizi Oil Layer in Qijia Area as an Example*; Northeast Petroleum University: Daqing, China, 2017.
57. Su, N. *Research on the Characteristics and Genesis of Ultra-low Permeability Sandstone Reservoir of Chang. 8 in Heshui Area of Ordos Basin*; Northwestern University: Xi'an, China, 2007.
58. Ying, F. *The Division of Diagenetic Stages in Clastic Rocks*; Petroleum Industry Press: Beijing, China, 2003; p. 15.
59. Chen, J.; Yao, J.; Mao, Z.; Li, Q.; Luo, A.; Deng, X.; Shao, X. Sedimentary and diagenetic controls on reservoir quality of low-porosity and low-permeability sandstone reservoirs in Chang10(1), Upper Triassic Yanchang Formation in the Shanbei area, Ordos Basin, China. *Mar. Pet. Geol.* **2019**, *105*, 204–221. [CrossRef]
60. Rossi, C.; Kälin, O.; Arribas, J.; Tortosa, A. Diagenesis, provenance and reservoir quality of Triassic TAGI sandstones from Ourhoud field, Berkine (Ghadames) Basin, Algeria. *Mar. Pet. Geol.* **2002**, *19*, 117–142. [CrossRef]
61. Morad, S.; Al-Ramadan, K.; Ketzer, J.M.; de Ros, L.F. The impact of diagenesis on the heterogeneity of sandstone reservoirs: A review of the role of depositional facies and sequence stratigraphy. *Am. Assoc. Pet. Geol. Bull.* **2010**, *94*, 1267–1309. [CrossRef]
62. Morad, S. *Carbonate Cementation in Sandstones: Distribution Patterns and Geochemical Evolution*; Blackwell Publishing Ltd.: Hoboken, NH, USA, 2009.
63. Irwin, H.; Curtis, C.; Coleman, M. Isotopic evidence for source of diagenetic carbonates formed during burial of organic-rich sediments. *Nature* **1977**, *269*, 209–213. [CrossRef]
64. Siegel, D.I.; Lesniak, K.A.; Stute, M.; Frape, S. Isotopic geochemistry of the Saratoga springs: Implications for the origin of solutes and source of carbon dioxide. *Geology* **2004**, *32*, 257–260. [CrossRef]
65. Sun, G.Q.; Wang, H.F.; Zou, K.Z.; Wang, W.Z. Characteristics and significance of carbon and oxygen isotopic compositions of carbonate cements in Jiulongshan region, North Edge of Qaidam Basin. *Nat. Gas. Geosci.* **2014**, *25*, 1358–1365.
66. Fu, S.; Wang, Z.; Zhang, Y.; Wang, A.; Kong, H.; Fang, C. Origin of carbonate cements in reservoir rocks and its petroleum geologic significance: Eboliang structure belt, northern margin of Qaidam Basin. *Acta Sedimentol. Sin.* **2015**, *33*, 991–999.
67. Li, Q.; Jiang, Z.; Liu, K.; Zhang, C.; You, X. Factors controlling reservoir properties and hydrocarbon accumulation of lacustrine deep-water turbidites in the Huimin Depression, Bohai Bay Basin, East China. *Mar. Pet. Geol.* **2014**, *57*, 327–344. [CrossRef]
68. Zhong, D.K.; Zhu, X.M. Characteristics and genetic mechanism of deep-buried clastic eureservoir in China. *Sci. China Ser. D* **2008**, *51*, 11–19. [CrossRef]
69. Surdam, R.C.; Crossey, L.J.; Hagen, E.S.; Heasler, H.P. Organic-inorganic interactions and sandstone diagenesis. *Am. Assoc. Pet. Geol. Bull.* **1989**, *73*, 1–23.
70. Zhao, X. *Clay Mineral and Application in Oil and Gas Exploration and Development*; China Ocean Press: Beijing, China, 2012; p. 424.
71. Mansurbeg, H.; Morad, S.; Salem, A.; Marfil, R.; El-Ghali, M.A.K.; Nystuen, J.P.; Caja, M.A.; Amorosi, A.; Garcia, D.; La Iglesia, A. Diagenesis and reservoir quality evolution of palaeocene deep-water, marine sandstones, the Shetland-Faroes Basin, British continental shelf. *Mar. Pet. Geol.* **2008**, *25*, 514–543. [CrossRef]
72. Surdam, R.C.; Boese, S.W.; Crossey, L.J. The Chemistry of Secondary Porosity. *Am. Assoc. Pet. Geol. Bull. Mem* **1984**, *37*. [CrossRef]
73. Yuan, G.; Gluyas, J.; Cao, Y.; Oxtoby, N.H.; Jia, Z.; Wang, Y.; Xi, K.; Li, X. Diagenesis and reservoir quality evolution of the Eocene sandstones in the northern Dongying Sag, Bohai Bay Basin, East China. *Mar. Petr. Geol.* **2015**, *62*, 77–89. [CrossRef]
74. Zhou, G.; Chen, Q.; Cui, G.; Wang, G.; Wang, Y. Geological characteristics and main controlling factors of Paleogene-Neogene gas reservoir in the east of the Altun Mountains in the Qaidam Basin. *J. Northwest Univ.* **2018**, *48*, 115–122.
75. Worden, R.H.; Burley, S.D. *Sandstone Diagenesis: The Evolution of Sand to Stone*; Blackwell Publishing Ltd.: Hoboken, NH, USA, 2009.
76. Zheng, J.; Ying, F. Reservoir characteristics and diagenetic model of sandstone intercalated in coal-bearing strata (acid water medium). *Acta Patrolei. Sin.* **1997**, *18*, 19–24.
77. Hower, J.; Eslinger, E.V.; Hower, M.E.; Perry, E.A. Mechanism of burial metamorphism of argillaceous sediment: 1. Mineralogical and chemical evidence. *Geol. Soc. Am. Bull.* **1976**, *87*, 725–737. [CrossRef]
78. Zhu, H.H.; Zhong, D.K.; Yao, J.L.; Sun, H.T.; Niu, X.B.; Liang, X.W.; You, Y.; Li, X. Alkaline diagenesis and its effects on reservoir porosity: A case study of Upper Triassic Chang 7 Member tight sandstone in Ordos Basin, NW China. *Pet. Explor Dev.* **2015**, *42*, 56–65. [CrossRef]
79. Chang, X.; Wang, Y.; Shi, B.; Xu, Y. Charging of carboniferous volcanic reservoirs in the eastern Chepaizi uplift, Junggar Basin (northwestern China) constrained by oil geochemistry and fluid inclusion. *Am. Assoc. Pet. Geol. Bull.* **2019**, *103*, 1625–1652. [CrossRef]

80. Lai, J.; Wang, G.W.; Fan, Z.Y.; Wang, Z.Y.; Chen, J.; Zhou, Z.L.; Wang, S.C.; Xiao, C.W. Fracture detection in oil-based drilling mud using a combination of borehole image and sonic logs. *Mar. Pet. Geol.* **2017**, *84*, 195–214. [CrossRef]
81. Yuan, Z. *Study on the Characteristics and Control. Factors Analysis of Oil& Gas. Reservoir of the Upper Triassic in Southeast. Ordos Basin*; Northwestern University: Xi'an, China, 2011.